Reactions of $Fe(CO)_3$ and $Fe(CO)_4$ with C_2Cl_4 in the Gas Phase Monitored by Transient Infrared Spectroscopy: Formation of $Fe(CO)_4(C_2Cl_4)$, $Fe(CO)_3(C_2Cl_4)_2$, and Novel Chloride Complexes Resulting from the Oxidative Addition of C_2Cl_4

David L. Cedeño and Eric Weitz*

Department of Chemistry, Northwestern University, Evanston, Illinois 60208-3113

Received: March 29, 2000; In Final Form: June 16, 2000

The gas-phase reactions of $Fe(CO)_3$ and $Fe(CO)_4$ with perchloroethylene (C_2Cl_4) have been investigated using transient infrared spectroscopy. The addition of C_2Cl_4 to $Fe(CO)_3$ produces $Fe(CO)_3(C_2Cl_4)$ with a rate constant of $(3.0 \pm 0.8) \times 10^{-11}$ cm^3 molecule^{-1} s^{-1}. A second olefin can add to $Fe(CO)_3(C_2Cl_4)$ with a rate constant of $(1.9 \pm 0.3) \times 10^{-13}$ cm^3 molecule^{-1} s^{-1} to form the novel bisolefin complex $Fe(CO)_3(C_2Cl_4)_2$. Absorptions of this complex were identified at 2084 and 2057 cm^{-1}. C_2Cl_4 reacts with $Fe(CO)_4$ with a rate constant of $(1.2 \pm 0.3) \times 10^{-13}$ cm^3 molecule^{-1} s^{-1} to produce $Fe(CO)_4(C_2Cl_4)$, which is identified by its absorptions at 2125, 2069, and 2039 cm^{-1}. This product isomerizes to a novel chloride complex via an oxidative addition process, with Arrhenius parameters $E_a = 21 \pm 2$ kcal/mol and $\ln A = 28 \pm 2$ in the 297−315 K temperature range. The chloride complex is best assigned as $ClFe(CO)_4(C_2Cl_3)$, and possible mechanisms for this isomerization reaction are discussed. $ClFe(CO)_4(C_2Cl_3)$ can also be produced by the photolysis of $Fe(CO)_4(C_2Cl_4)$, and a mechanism for this process is proposed. Absorptions of $ClFe(CO)_4(C_2Cl_3)$ were identified at 2166, 2109, and 2089 cm^{-1}. Where possible, the measured rate constants and the observed infrared absorptions are compared to those for analogous C_2H_4 and C_2F_4 complexes. Finally, simulations of a "global" mechanism for the kinetics of this system are in good agreement with experimental data. From these simulations, ΔG for the isomerization of $Fe(CO)_3(C_2Cl_4)$ to $ClFe(CO)_3(C_2Cl_3)$ is estimated to be ≥ 4 kcal/mol at 297 K.

I. Introduction

Transition metal carbonyls with olefins as ligands are crucial intermediates in catalytic cycles for processes such as olefin isomerization, hydrogenation, hydrosilation, and hydroformylation.[1−4] The stability and reactivity of metal carbonyl complexes play an important role in the product distribution and yields of such chemical processes.[5] Both the physical and chemical properties of these complexes are dependent on ligand−metal interactions. For alkenes, these can depend on the nature of the substituents around the double bond. In the context of the Dewar−Chatt−Duncanson model,[6,7] the olefin donates electron density from its π orbital, while the metal is able to back-donate electron density into the empty π^* orbital of the olefin. Thus, the stability of 18-electron olefin complexes is related to the ability of the olefin to donate electron density to the metal along with its ability to accept electron density from the metal. Other bound ligands can have an effect on the availability and apportioning of electron density from olefins. Additionally, strong electron-withdrawing substituents such as the halogens or the cyano moiety can lead to a decrease in the electron density available from an olefin for σ donation. In this case, there is a concomitant decrease in electron density available for back-bonding. However, the indicated substituents make the olefin a better electron acceptor. Interactions of this type would be expected to have an effect on the metal−ligand bond energy.

Mono and bis metal carbonyl−olefin complexes can be generated in the gas phase by the addition of an alkene to a coordinatively unsaturated species that has been produced by the photolytic loss of CO from a metal carbonyl precursor.[8] Rate constants for the addition of olefins to coordinatively unsaturated metal carbonyls can be measured using transient infrared laser spectroscopy (TILS)[8,9] by probing the CO stretching modes of a coordinatively unsaturated metal carbonyl and/or the product of such a reaction. These modes are very sensitive to the electronic environment around the metal. TILS and/or FTIR [or time-resolved FTIR (TRFTIR)] spectroscopy are methods that can be used to monitor the dissociation of suitable resulting 18-electron olefin complexes. Monitoring the dissociation kinetics under appropriate conditions can lead to a determination of the bond dissociation energy (BDE) for the complex under study.[9]

House and Weitz[10] estimated the BDE for bisethylene tricarbonyl iron and established lower limits for BDE's in the monoethylene and both corresponding tetrafluoroethylene complexes. DFT calculations[11] indicate that the BDE for the monoolefin complexes of ethylene and tetrafluoroethylene should be larger than the BDE for the perchloroethylene monoolefin analogue. Although the stronger back electron donation from the metal to the ligand, relative to that for ethylene, should be the dominant stabilizing effect for haloolefins, the deformation of the halogenated olefins and the iron tetracarbonyl fragment, possibly because of larger substitutent atoms on the olefin, could make the haloolefin complexes less stable relative to the ethylene complex.

House and Weitz[10] also observed that the rate constants for the addition of ethylene to both iron tetracarbonyl and iron tricarbonyl are larger than the corresponding rate constants for the addition of tetrafluoroethylene. An increase in the size of the substituents around the double bond could lead to unfavorable steric effects on the rate constant for the binding of a ligand to a metal carbonyl complex. Such steric effects could be further accentuated when a second perchloroethylene adds to a mo-

10.1021/jp0011894 CCC: $19.00
Published on Web 08/01/2000

noolefin tricarbonyl iron complex, especially when the monoolefin has very large substituent atoms, as does perchloroethylene. Chlorination of a metal as a result of the reaction of chloroethylenes with transition metal complexes has been reported for platinum,[12,13] manganese,[14] and iron[15−20] complexes in solution. Hazseldine and co-workers[15−17] reported the formation of a variety of monohaloethylene iron tetracarbonyl compounds as well as a qualitative determination of their stability. A discussion of possible decomposition paths for these complexes in solution is also provided. On the basis of mass spectrometric data they suggest that insertion of the metal into the C−X (X = Cl or Br) bond is occurring. Grevels and co-workers[18] reported the reaction of 1,2-dichloroethylene and nonacarbonyl diiron in solution to yield a diiron product containing a chlorine bridging the two metal atoms. They proposed a mechanism for the formation of this product in which there is migration of a chlorine from the olefin to the metal. However, they did not provide kinetic data related to the formation of such a product. Sloan and co-workers[19] report a similar process taking place as a result of the reaction of nonacarbonyl diiron with 2,3-dichlorobutadiene. A plausible explanation for the observed final reaction products involves an insertion of $Fe(CO)_4$ into a C−Cl bond after the formation of the $Fe(CO)_4(\eta^2$-diene) complex. A similar reaction has been reported by Lowe et al.,[20] which leads to $ClFe(CO)_2[P(OMe)_3]_2$-$[C{\equiv}CCH(O(CH_2)_3O)_2]$, in which $ClC{\equiv}CCH(O(CH_2)_3O)_2$ is the species undergoing oxidative addition.

In this paper, the reactions of tetrachloroethylene with unsaturated metal carbonyls have been studied with the objective of obtaining a better understanding of how the substituents on the olefin affect the bonding and the stability of olefin−metal complexes. Rate constants for addition of perchloroethylene to $Fe(CO)_3$, $Fe(CO)_4$, and $Fe(CO)_3(C_2Cl_4)$ were determined using TILS and compared to those obtained for the respective addition reactions of ethylene and tetrafluoroethylene.[10] One of the most interesting observations is that the monoolefin products, $Fe(CO)_n(C_2Cl_4)$ (n = 3 or 4) undergo oxidative addition of the olefin to form their respective chloride vinyl isomers $ClFe(CO)_n(C_2Cl_3)$, in which an olefinic C−Cl bond has been activated. Kinetic and spectroscopic evidence for C−Cl bond activation is presented in the context of a mechanism that is consistent with all of the experimental results.

II. Experimental Section

The apparatus used to monitor the species formed as a result of the interaction of C_2Cl_4 with unsaturated iron carbonyl species has been described previously.[8,9] Iron pentacarbonyl was photolyzed with the unfocused beam of a XeCl excimer laser (Questek, 308 nm). The output power of the laser was ∼7 mJ/cm^2 at the cell window and was delivered at a frequency of 1 Hz unless otherwise stated. Photolysis at 308 nm produces $Fe(CO)_3$ as the only detectable product.[21]

The infrared beam from a tunable diode laser (Laser Photonics), which was passed twice through a 42-cm cell that was terminated with CaF_2 windows was used to probe the kinetics of the association reactions. The IR laser beam was detected with a fast InSb detector (EG&G-Judson, $\tau_{1/2} \approx 70$ ns), the output of which was sent to either a Perry ×100 amplifier for the fastest transients or to a variable gain and variable bandwidth amplifier (SRS 560). The amplified signals were sent to a digital storage oscilloscope (Lecroy 9400) that averaged 20−40 events. The averaged signal was sent via a GPIB interface to a computer for further analysis. Rate constants were obtained from the slope of a plot of the rate of reaction versus ligand pressure.

Time-resolved infrared spectra can be constructed from the individual time traces taken over the desired probe frequency range. When a computer is used to connect a point from each transient at a common time delay, a spectrum at that time delay is generated. This procedure can be repeated for subsequent time points to produce a set of spectra that allow the time evolution of a reacting system to be followed.

For experiments above room temperature, the cell was wrapped with heating tape and insulated with fiberglass batting. Temperature control was achieved through a variable voltage transformer, while the temperature was monitored by the three chromel−alumel thermocouples attached to the outside of the cell. For temperatures below room temperature, a 42-cm water-jacketed cell was used. A thermostated chiller cooled water to the desired temperature, which was monitored using a precision thermometer (±0.05 °C). The temperature at the cell was ∼0.5−1.0 °C above the water bath temperature, as indicated by three chromel−alumel thermocouples attached to the external wall of the cooling jacket.

TILS experiments were performed over acquisitions times of 500 ms or less. The products of association reactions of unsaturated iron carbonyl species that yielded relatively stable products were studied using a FTIR spectrophotometer (Mattson, RS1) operating in the "GC" mode. In this mode, spectra of the cell contents could be acquired during and/or after photolysis at predetermined time intervals. Using this method, spectra were obtained in the 1900−2200 cm^{-1} region at 4 cm^{-1} resolution. In these experiments, gas mixtures were allowed to equilibrate for 30 min before excimer laser photolysis, typically using a 5-Hz pulse rate and 150−300 laser pulses.

Rate constants for ligand association reactions were measured under the following conditions in a static cell: for $Fe(CO)_3 + C_2Cl_4$, 0.080−0.090 Torr of $Fe(CO)_5$, 0.00−2.00 Torr of C_2Cl_4; for $Fe(CO)_4 + C_2Cl_4$; 0.080−0.085 Torr of $Fe(CO)_5$, 4.00 Torr of CO, 0.00−4.00 Torr of C_2Cl_4; for $Fe(CO)_3(C_2Cl_4) + C_2Cl_4$; 0.080−0.085 Torr of $Fe(CO)_5$, 0.00−4.00 Torr of C_2Cl_4; and for $Fe(CO)_3(C_2Cl_4)$ + CO; 0.080−0.085 Torr of $Fe(CO)_5$, 4.00 Torr of C_2Cl_4, 0.00−0.80 Torr of CO. Enough helium was added to attain a total pressure of at least 30 Torr. Experiments were performed to ensure that this corresponded to the high-pressure limit for these reactions.[8] Errors reported in the determination of rate constants are $\pm 2\sigma$ and are based solely on precision.

For FTIR experiments 0.04−0.05 Torr of $Fe(CO)_5$, 2.5−5.0 Torr of C_2Cl_4, and various amounts of CO (0.0−70.0 Torr) were used to adjust the CO/C_2Cl_4 ratio in the mixture. When necessary, helium was added to ensure that the total pressure was no less than ∼40 Torr.

$Fe(CO)_5$ was obtained from Aldrich and subjected to a series of freeze−pump−thaw cycles before use. At the beginning of each day, the iron pentacarbonyl was briefly freeze−pump−thawed to remove any CO and/or other volatile material that might be present because of decomposition. Tetrachloroethylene (99.9%) was purchased from Aldrich and, before use, was subjected to a series of three freeze−pump−thaw cycles. Carbon monoxide (Matheson, 99.995%) and helium (Linde or Air Products, 99.999%) were used as received.

III. Results

A. Reaction of $Fe(CO)_3$ and the $Fe(CO)_3$ Perchloroethylene Adduct with C_2Cl_4. Figure 1 shows time-resolved spectra obtained in the 2050−2100 cm^{-1} region at 4 cm^{-1} intervals from the photolysis of 0.08 Torr of $Fe(CO)_5$ and 3.5 Torr of C_2Cl_4 in the absence of added CO. It is clear that there is a

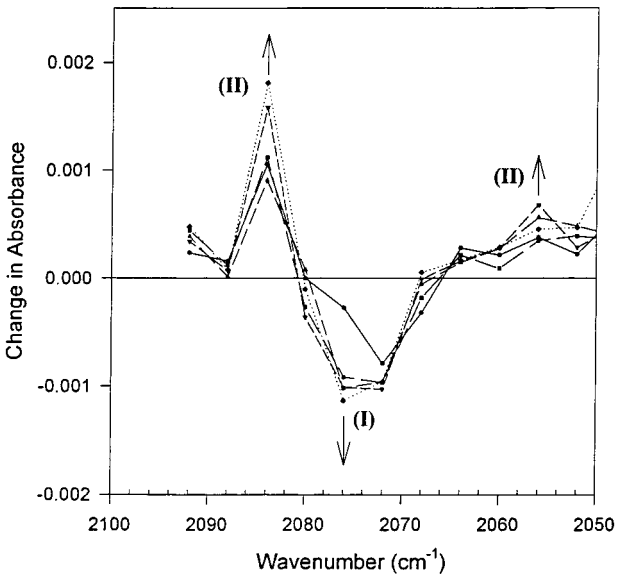

Figure 1. Time-resolved IR difference spectra produced following 308-nm laser photolysis of 85 mTorr of $Fe(CO)_5$, 3.5 Torr of C_2Cl_4, and 21 Torr of He. The spectra shown correspond to the 30−150 μs time range after photolysis and are displayed in 30 μs intervals. The spectrum obtained at 10 μs has been subtracted from each spectrum to compensate for the effect of parent depletion. The solid line marks the first time increment. The down arrow indicates the depletion of intermediate (**I**), and the up arrow indicates the growth of product (**II**).

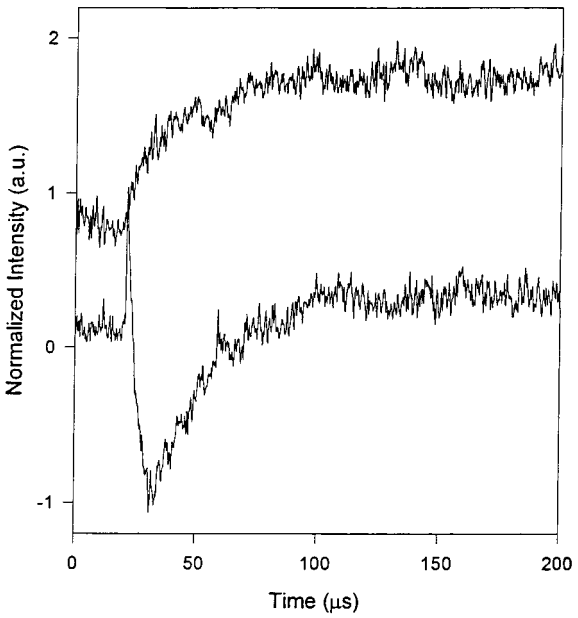

Figure 2. Transient signals showing the depletion (lower trace, inverted for comparison) of $Fe(CO)_4$ at 2000 cm^{-1} and growth (upper trace) of $Fe(CO)_4(C_2Cl_4)$ at 2072 cm^{-1} obtained following 308-nm photolysis of 85 mTor $Fe(CO)_5$, 4 Torr of C_2Cl_4, 10 Torr of CO, and 15 Torr of He.

species being depleted at ~2076 cm^{-1} while another species with absorptions around 2084 and 2057 cm^{-1} grows in. An isobestic point between the 2076 and 2084 cm^{-1} bands suggests that the change in absorbance of the bands belonging to these species is the result of a common chemical process. The rate of addition of C_2Cl_4 to $Fe(CO)_3$ was monitored using the $Fe(CO)_3$ absorption band at 1950 cm^{-1}.[21] Following the very rapid photolytic formation of $Fe(CO)_3$, a decay that depends on C_2Cl_4 pressure is observed. The absence of added CO and the dependence of this decay on C_2Cl_4 pressure suggests that the reaction that is occurring is

$$Fe(CO)_3 + C_2Cl_4 \rightarrow Fe(CO)_3(C_2Cl_4) \qquad (1)$$

and thus the species that has an absorption at 2076 cm^{-1} is $Fe(CO)_3(C_2Cl_4)$. However, as discussed in more detail in section IV.D, it is conceivable that this complex, which we designate as species **I**, is an isomer of $Fe(CO)_3(C_2Cl_4)$ that can result from a rapid chlorine atom transfer to the metal atom, as shown in eq 2.

$$Fe(CO)_3(C_2Cl_4) \rightleftharpoons ClFe(CO)_3(C_2Cl_3) \qquad (2)$$

To our knowledge, there are no literature reports of the spectra for either of these two species, so the identity of the species **I** cannot be assigned without further analysis of the kinetic and spectroscopic data (*vide infra*).

A plot of the rate of addition of C_2Cl_4 to $Fe(CO)_3$ versus the pressure of C_2Cl_4 yields a rate constant of $(3.0 \pm 0.8) \times 10^{-11}$ cm^3 $molecule^{-1}$ s^{-1} at 24 °C. This rate constant is temperature-independent (within experimental error) in the 4−37 °C range. The rate of rise of **I** at 2076 cm^{-1} vs olefin pressure gives a rate constant of $(2 \pm 1) \times 10^{-11}$ cm^3 $molecule^{-1}$ s^{-1}. Rates for formation of species **I**, probed at 2076 cm^{-1}, were difficult to measure, as this band is convoluted with the fast photolytic decay of $Fe(CO)_5$, which has an absorption in this region. Nevertheless, the rate constant determined from measurements at 2076 cm^{-1} is within experimental error of that determined from measurements at 1950 cm^{-1}.

Bands at 2084 and 2057 cm^{-1} grow at the expense of the absorption at 2076 cm^{-1}. This behavior implies that these bands belong to a new species (**II**) that is the product of the addition a second olefin molecule to species **I**. Species **II** could be either $Fe(CO)_3(C_2Cl_4)_2$ or $ClFe(CO)_3(C_2Cl_3)(C_2Cl_4)$, depending on the identity of species **I**. Any other bands that might be in the region between ~2036 and 2000 cm^{-1} would be convoluted with bands from parent and polynuclear species in this region, making their identification and assignment difficult. Because the diode laser used in these experiments did not produce useful output above 2120 cm^{-1}, any absorption(s) above this frequency could not be probed. The rate constant for addition of perchloroethylene to species **I** was determined to be $(1.9 \pm 0.3) \times 10^{-13}$ cm^3 $molecule^{-1}$ s^{-1} at 24 °C by monitoring the decay of its 2076 cm^{-1} absorption. The rise of the product absorption at 2084 cm^{-1} yielded a rate constant of $(1.8 \pm 0.6) \times 10^{-13}$ cm^3 $molecule^{-1}$ s^{-1}, giving an error-weighted average rate constant of $(1.9 \pm 0.3) \times 10^{-13}$ cm^3 $molecule^{-1}$ s^{-1}. This rate constant is temperature-independent within experimental error in the 4−37 °C range. The CO pressure dependence of the rate of loss of species **I** at 2076 cm^{-1} yielded a rate constant of $(2.4 \pm 0.7) \times 10^{-12}$ cm^3 $molecule^{-1}$ s^{-1} at 24 °C for addition of CO to this unsaturated species.

B. Reaction of $Fe(CO)_4$ with C_2Cl_4. Although laser photolysis of $Fe(CO)_5$ at 308 nm yields $Fe(CO)_3$ as the only detectable product,[21] in the presence of sufficient CO, $Fe(CO)_3$ can add CO ($k = 2.2 \times 10^{-11}$ cm^3 $molecule^{-1}$ s^{-1}) to produce $Fe(CO)_4$. When this occurs in the presence of C_2Cl_4, the C_2Cl_4 can add to $Fe(CO)_4$ to yield a saturated 18-electron complex. Figure 2 shows typical transient signals for this process. The lower trace, which has been inverted for comparison purposes, is due to the depletion of $Fe(CO)_4$, as a result of the reaction of $Fe(CO)_4$ and C_2Cl_4 to form an adduct designated as species **III**. The rising portion of this trace (before inversion) is due to the formation of $Fe(CO)_4$ from $Fe(CO)_3 + CO$, while the initial very fast depletion (before inversion), which precedes the rise,

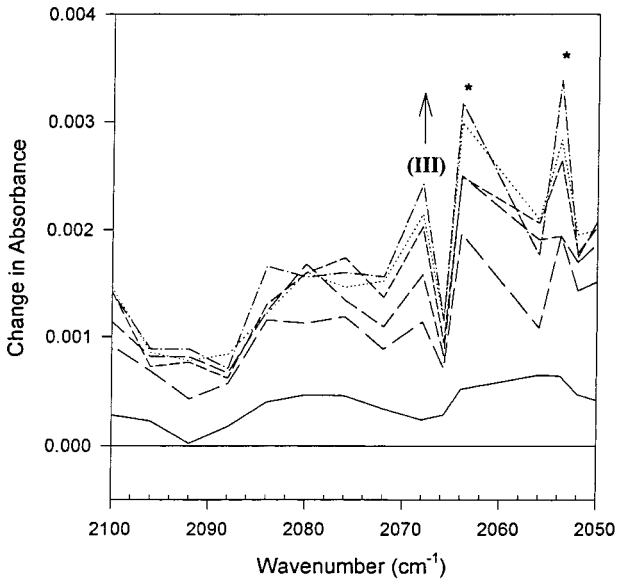

Figure 3. Time-resolved IR difference spectra produced following 308-nm laser photolysis of 90 mTorr of $Fe(CO)_5$, 2.2 Torr of C_2Cl_4, 10 Torr of CO, and 15 Torr of He. The spectra are shown in 6 μs intervals over the 4−34 μs time range after photolysis. The spectrum obtained at 2 μs has been subtracted from each spectrum to compensate for parent depletion. The solid line marks the first time increment. The arrow indicates the growth of an $Fe(CO)_4(C_2Cl_4)$ absorption. Asterisks denote absorptions bands of polynuclear products.

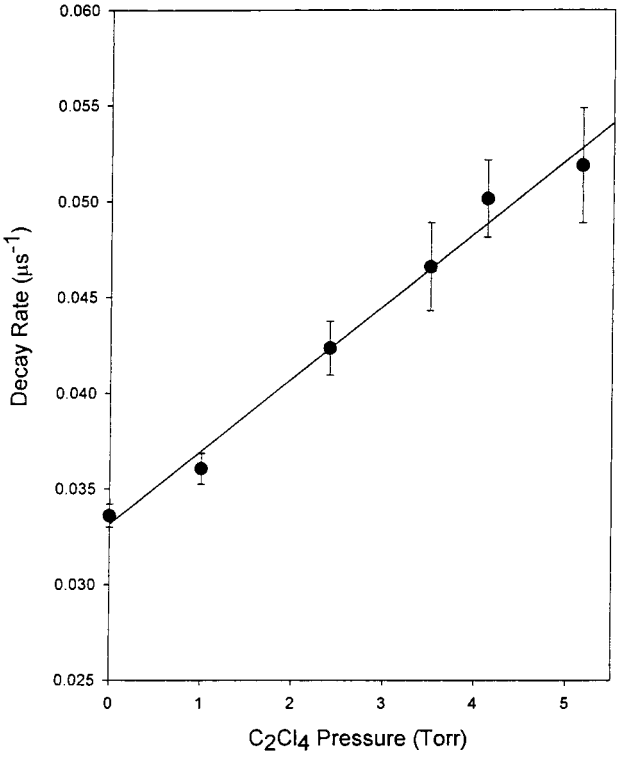

Figure 4. Plot of the rate of decay of the $Fe(CO)_4$ absorption band at 2000 cm^{-1} as a function of the C_2Cl_4 pressure.

is due to photolytic depletion of $Fe(CO)_4$ and/or $Fe(CO)_5$ [an absorption of $Fe(CO)_5$ overlaps the 2000 cm^{-1} $Fe(CO)_4$ absorption]. The upper trace shows the growth of species **III** monitored at 2072 cm^{-1}. From the figure, it is obvious that, as expected, the rates for these processes agree.

Figure 3 shows time-resolved spectra obtained in the 2050−2100 cm^{-1} region, at 4 cm^{-1} intervals, after photolysis of 0.09 Torr of $Fe(CO)_5$, 2.2 Torr of C_2Cl_4, and 10 Torr of CO. Absorptions that appear in the 2050−2064 cm^{-1} region have been previously identified as belonging to polynuclear species that are formed by the reaction of unsaturated iron species and parent.[22] The band at 2052 cm^{-1} is due to $Fe_2(CO)_8$, while the band at 2066 cm^{-1} belongs to $Fe_2(CO)_9$.[22] The band growing in at ∼2070 cm^{-1} corresponds to a new species, **III**, which lives for more than 500 ms. No other absorptions of species **III** have been detected using the diode laser probe. However, as discussed below two other absorptions were observed for species **III** using the FTIR. One of these is at 2125 cm^{-1} which is out of the range of operation of the diode laser used in these studies and the other is at 2039 cm^{-1}. This latter absorption both is weaker than the absorption that was monitored with the diode laser at 2069 cm^{-1} and overlaps a region of the spectrum where $Fe(CO)_5$ absorbs.

A plot of the rate of loss of iron tetracarbonyl vs perchloroethylene pressure, monitored at 2000 cm^{-1}, is shown in Figure 4 and yields a rate constant of $(1.2 \pm 0.2) \times 10^{-13}$ cm^3 $molecule^{-1}$ s^{-1}. The plot of the rise of the product absorption at 2072 cm^{-1} vs C_2Cl_4 pressure gives a rate constant of $(1.8 \pm 0.5) \times 10^{-13}$ cm^3 $molecule^{-1}$ s^{-1} at 24 °C. These measurements yield an error-weighted average rate constant of $(1.2 \pm 0.3) \times 10^{-13}$ cm^3 $molecule^{-1}$ s^{-1}. This rate constant is temperature-independent within experimental error in the 4−37 °C range.

As indicated below, species **III** was also observed using TRFTIR. Post-photolysis FTIR spectra in the 1900−2200 cm^{-1} region reveal the presence of product absorptions at frequencies above the parent region, as would be expected for an olefin

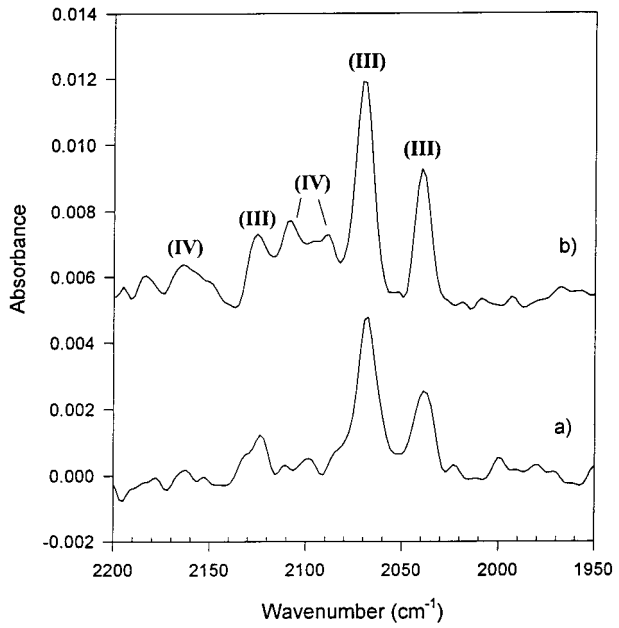

Figure 5. FTIR spectra acquired after 300 laser pulses (308 nm), which photolyzed (a) a mixture containing 50 mTorr of $Fe(CO)_5$, 4.8 Torr of C_2Cl_4, 9.8 Torr of CO, and 24 Torr of He and (b) a mixture containing 40 mTorr of $Fe(CO)_5$, 4.9 Torr of C_2Cl_4, and 35 Torr of CO. A scaled spectrum of $Fe(CO)_5$ has been added to each of the spectra to account for parent depletion that occurs as a result of photolysis.

ligand with electron-withdrawing substituents. Figure 5a shows a typical FTIR spectrum obtained after photolysis of 0.05 Torr of $Fe(CO)_5$, 4.8 Torr of C_2Cl_4, and 9.8 Torr of CO. Three bands belonging to species **III** were observed at 2039, 2069, and 2125 cm^{-1}, with relative peak intensities of approximately 0.73, 1.00, and 0.45, respectively. Species **III** can be assigned as $Fe(CO)_4(C_2Cl_4)$ on the basis of the previously reported spectra for this compound obtained by Haszeldine et al.[16] with bands at 2004

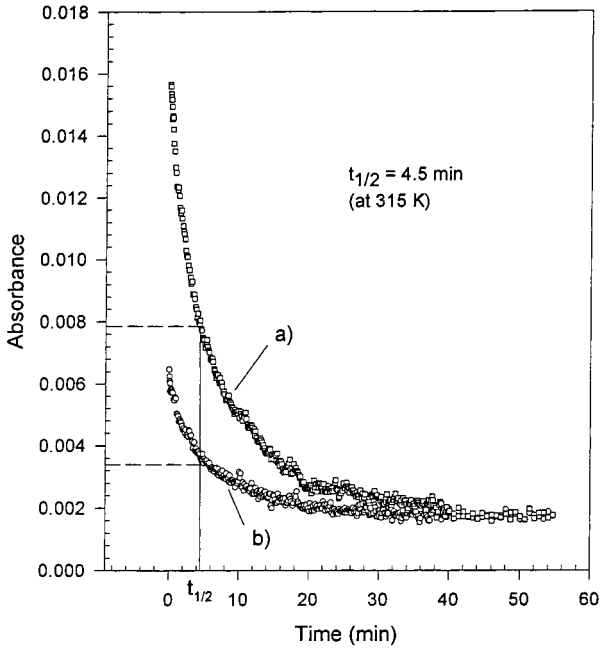

Figure 6. Decay of $Fe(CO)_4(C_2Cl_4)$ as a function of the ratio of C_2Cl_4 to CO at 315 K: (a) $C_2Cl_4/CO = 28$ and (b) $C_2Cl_4/CO = 2.0$.

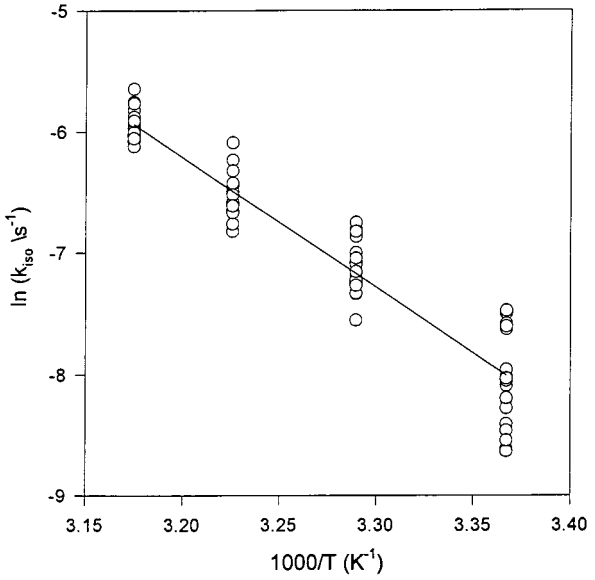

Figure 7. Arrhenius plot for the isomerization of $Fe(CO)_4(C_2Cl_4)$ to $ClFe(CO)_3(C_2Cl_3)$ in the 297−315 K temperature range. The line is the result of an unweighted fit of all the data.

(w), 2040 (s), 2072 (vs), and 2134 (s) cm^{-1} with hexanes as the solvent. The 2004 cm^{-1} band overlaps the parent region and was not observed in the present study, even after subtraction of the parent absorption. This is presumably due to the fact that the 2004 cm^{-1} absorption is the weakest of the reported absorptions for this compound and that the signal-to-noise level in these experiments is degraded as a result of subtraction. As expected, the intensity of this set of bands increases if either the CO or the ligand pressure is increased with the other being held constant, at least for CO pressures >2 Torr and ligand pressures >1 Torr. $Fe(CO)_4(C_2Cl_4)$ is fairly stable, decomposing on a time scale of approximately 3 h at room temperature. However, there is no FTIR evidence for gas-phase product(s) growing in on this time scale.

The dependence of the rate of decay of the absorption band at 2069 cm^{-1} on different CO/C_2Cl_4 ratios was probed using FTIR to determine whether a dissociative mechanism for loss of olefin was the dominant path for decomposition of $Fe(CO)_4(C_2Cl_4)$. The decay of $Fe(CO)_4(C_2Cl_4)$ is single-exponential except at low CO/C_2Cl_4 pressure ratio (<2) and at temperatures below 304 K, where the decay becomes biexponential. The amplitude of the fast component in the biexponential decay decreases as either the temperature or the CO/C_2Cl_4 pressure ratio is increased. Fits of the biexponential signals at different CO/C_2Cl_4 ratios gave rates for the fast decay in the $(3-11) \times 10^{-3}$ s^{-1} range. However, the error in these fits is in the 20−70% range, with the largest errors being for those rates measured at larges CO/C_2Cl_4 ratios and higher temperatures. The magnitude of the uncertainty in the rate of the fast decay precluded an accurate determination of the dependence of the fast decay on the CO/C_2Cl_4 ratio and on the temperature. On the other hand, both the rate for the slow component of the biexponential decay of $Fe(CO)_4(C_2Cl_4)$ and the rate of the single-exponential decay observed at higher CO/C_2Cl_4 ratios (>2) and temperatures *are independent of the CO, olefin, and parent pressures* within experimental error (Figure 6). However, they are temperature-dependent and give a linear Arrhenius plot (Figure 7) in the 297−315 K range. Treating this decay process as an elementary first-order reaction, the data in Figure 7 lead to a preexponential factor, $\ln A = 28 \pm 2$ (A in s^{-1}) and an activation energy, $E_a = 21 \pm 2$ kcal mol^{-1}. The change in the appearance of the decay with both temperature and CO pressure indicates that the mechanism for decomposition of $Fe(CO)_4(C_2Cl_4)$ can involve multiple pathways. These pathways will be discussed in more detail in section IV.G.

Interestingly, the FTIR spectrum changes appearance as a function of the amount of added CO. When 35.0 Torr of CO is present in the photolysis cell (Figure 5b), a new set of absorptions appears in addition to those for $Fe(CO)_4(C_2Cl_4)$. These new absorptions consist of a broad feature, which is the convolution of two absorptions centered at ∼2089 and ∼2109 cm^{-1}, along with a band at 2166 cm^{-1}. This second set of absorptions decays much faster than those of the $Fe(CO)_4(C_2Cl_4)$. The intensity of the second set of bands, at 2089 (0.8), 2109 (1.0), and 2166 (0.2) cm^{-1}, increases with increasing CO pressure, suggesting that this species **(IV)** comes from the addition of CO to an unsaturated intermediate. Because the photolysis experiments are conducted in a static cell, it is also possible that species **IV** forms as a result of photolysis of $Fe(CO)_4(C_2Cl_4)$. This possibility will be discussed further in section IV.C. The absorbance of the bands assigned to species **IV** increases when the photolysis time is increased. FTIR spectra taken during photolysis show that species **IV** only starts to form after some $Fe(CO)_4(C_2Cl_4)$ has been formed. There is an induction period of approximately 20 photolysis shots that is independent of the laser repetition rate (0.5−5 Hz). Diode laser experiments that probed the 2089 and 2109 cm^{-1} absorptions confirmed the formation of species **IV** when more than ∼10 Torr of CO was present in the photolysis cell. Both the intensity and rate of growth of the signal increased with an increase in the CO pressure above 10 Torr.

The carbonyl stretching bands of species **IV** are displaced to higher energy relative to those of $Fe(CO)_4(C_2Cl_4)$. As will be discussed in more detail in section IV.C, there is evidence suggesting that species **IV** is a chloride complex, probably $ClFe(CO)_4(C_2Cl_3)$. To our knowledge, this compound has not been previously reported and thus there is no spectroscopic data available for it.

Although, in principle, species **IV** could be the bisolefin product, $Fe(CO)_3(C_2Cl_4)_2$, its formation would then expected to become *less favorable* at high CO pressure, contrary to what

is observed. The concentration of any species containing two haloolefin units should decrease as the CO pressure is increased because CO will compete for addition to the unsaturated precursor formed by the addition of C_2Cl_4 to $Fe(CO)_3$.

Another possibility is that species **IV** is *cis*-$Fe(CO)_4(Cl)_2$, which absorbs at 2164 (0.19), 2124 (1.00), 2108(0.77), and 2084 (0.85) cm^{-1} in a tetrachloroethylene solution.[23] This compound could be formed if the first chlorine atom transfer reaction is followed by another chlorine atom transfer process that occurs in concert with the elimination of dichloroacetylene.

$$Fe(CO)_4(C_2Cl_4) \rightarrow ClFe(CO)_4(C_2Cl_3) \quad (3)$$

$$ClFe(CO)_4(C_2Cl_3) \rightarrow Fe(CO)_4(Cl)_2 + C_2Cl_2 \quad (4)$$

A similar reaction has been observed by Amouri et al. for an iridium complex.[24] The main difference between $Fe(CO)_4(Cl)_2$ and $ClFe(CO)_4(C_2Cl_3)$ is that, in the dichloride a chlorine ligand replaces the trichlorovinyl ligand. It is not implausible that the effect of two chlorine ligands would result in a shift in the carbonyl stretching frequency similar to that caused by a chlorine plus a highly chlorinated vinyl ligand. However, if species **IV** is the cis dichloride, we would anticipate, on the basis of its solution spectrum, that it should have a strong absorption in the gas phase near 2125 cm^{-1}. Even though this absorption overlaps the absorptions of the monoolefin adduct, we would anticipate that it would be detectable, as it is expected to decay on a different time scale than the monoolefin. However, there was no obvious change in shape of bands in the 2125 cm^{-1} region when species **IV** was present versus when it was not present. Traces in the 2125 cm^{-1} region were carefully examined to determine whether they contained a more rapidly decaying component that could be attributed to species **IV**. Neither a change in shape nor a more rapidly decaying component was observed. These observations mitigate against the production of iron tetracarbonyldichloride. Conceivably, the relative intensity of the absorption bands in the gas phase versus solution could change, but there is no obvious reason for a dramatic change in intensity to occur. However, the iron carbonyl halides are photolabile,[23a,25] isomerizing to the trans isomer and then decomposing through the loss of CO. Therefore, it is possible that, under the conditions that lead to the production of species **IV**, a mixture of both dichloride isomers is present. If a mixture were present, the intensity pattern could be different than that reported for the cis dichloride. However, *a priori* one would anticipate that the lifetime of these two dichloride isomers would be different, leading to a time-dependent change in the intensity of their absorptions. This was not observed. Judging from these observations, we do not believe the dichloride is produced in these experiments. However, we do not feel we can completely rule out the possibility of its production.

Species **IV** survives for a shorter time than $Fe(CO)_4(C_2Cl_4)$, decaying thermally in about 10 min at room temperature. No bands were detected that grow at the rate of decay of species **IV**. An Arrhenius plot of the temperature dependence of this rate gives a preexponential factor $\ln A = 7.1 \pm 3.4$ and an activation energy $E_a = 7.2 \pm 2.0$ kcal mol^{-1}. Such small values for the preexponential factor and activation energy for this reaction suggest that the disappearance of species **IV** could involve a multiple-step pathway or heterogeneous processes on the cell walls. There is no indication that the decay is pressure-dependent, at least at CO pressures larger than 25 Torr, where the error in the determination of the decay rate is minimized. Section IV.C provides a further discussion of species **IV** and concludes that it is, indeed, most likely $ClFe(CO)_4(C_2Cl_3)$.

C. Polynuclear Formation. As seen in Figure 3, reactions of unsaturated species with parent to form polynuclear species compete with the addition of ligands to unsaturated species. Ryther and Weitz[22] established that the reaction of $Fe(CO)_5$ with $Fe(CO)_3$ has a rate constant that is near gas kinetic and results in $Fe_2(CO)_8$, which absorbs at 2052 cm^{-1}. In the absence of olefin, this polynuclear species decays slowly. The rate of decay of $Fe_2(CO)_8$ increases with the tetrachloroethylene pressure, as would be expected for an addition reaction. Although we cannot eliminate the possibility that the addition of a ligand is followed by an elimination reaction, prior studies suggest that an adduct with the formula $Fe_2(CO)_8(C_2Cl_4)$ is most likely.[22] The rate constant for this addition reaction is $(4.4 \pm 2.5) \times 10^{-14}$ cm^3 $molecule^{-1}$ s^{-1} at 24 °C. As expected, the addition of olefin decreases the intensity of the polynuclear signal because both the olefin and the parent compete for the available $Fe(CO)_3$. Thus, a large excess of olefin will inhibit the formation of polynuclear product. However, the vapor pressure of C_2Cl_4 limits its maximum pressure to ~5 Torr near room temperature.

$Fe(CO)_3(C_2Cl_4)$, obtained upon addition of olefin to $Fe(CO)_3$, also reacts with $Fe(CO)_5$. This reaction occurs in competition with the reaction of species **I** with C_2Cl_4. The rate constant for the reaction of parent with species **I** can be determined from the intercept of the C_2Cl_4 pressure-dependent plot for the decay of species **I**. For an $Fe(CO)_5$ concentration of 0.07 ± 0.01 Torr, the intercept of $(2.2 \pm 0.2) \times 10^{-2}$ μs^{-1} leads to a rate constant (k_p) for the reaction of parent with species **I** of $(9.7 \pm 3.5) \times 10^{-12}$ cm^3 $molecule^{-1}$ s^{-1} at 24 °C.

IV. Discussion

A. The Thermal Decay of $Fe(CO)_4(C_2Cl_4)$: An Oxidative Addition Reaction. The shape of the decay signal for $Fe(CO)_4(C_2Cl_4)$ depends on the temperature and the CO/C_2Cl_4 pressure ratio. When the CO/C_2Cl_4 ratio is above 2, the decay is a single exponential over the temperature range studied and, as can be seen in Figure 6, within experimental error, this single-exponential decay rate (k_{obs}) is independent of the CO/C_2Cl_4 pressure ratios in the 2.0−28 range.

An obvious possibility for the decay of $Fe(CO)_4(C_2Cl_4)$ is ligand loss or substitution. As has been shown in past studies of the determination of the BDE of ligands undergoing dissociative loss from metal carbonyl complexes, the observed rate of loss of the complex is dependent on the CO/ligand ratio.[10,26] When olefin tetracarbonyl iron complexes undergo dissociative olefin loss and excess CO is present in the reaction mixture, CO can add to the vacant coordination site.

$$Fe(CO)_4L \rightarrow Fe(CO)_4 + L \quad (k_d) \quad (5)$$

$$Fe(CO)_4 + L \rightarrow Fe(CO)_4L \quad (k_L) \quad (6)$$

$$Fe(CO)_4 + CO \rightarrow Fe(CO)_5 \quad (k_{CO}) \quad (7)$$

Using the steady-state approximation for the $Fe(CO)_4$ intermediate, the decay rate for such a process has been shown to be[9]

$$k_{obs} = (k_d k_{CO}[CO])/(k_L[L] + k_{CO}[CO]) \quad (8)$$

Thus, if dissociative ligand loss were occurring from $Fe(CO)_4(C_2Cl_4)$, larger CO/C_2Cl_4 ratios would increase the decay rate of $Fe(CO)_4(C_2Cl_4)$, which, at sufficiently large ratios, would approach the rate constant for dissociation, k_d. In the mechanism shown in reactions 5−7, k_{obs} will appear to be independent of changes in the ligand/CO ratio or ligand and CO pressures *only*

if $k_{CO}[CO] \gg k_L[L]$. In that case, eq 8 will reduce to $k_{obs} = k_d$. Judging from eq 8, a change in the CO/C_2Cl_4 ratio from 2.0 to 28 would lead to a change in k_{obs} from 0.87 k_d to 0.49 k_d. No change in k_{obs} was seen when the CO/C_2Cl_4 ratio was changed over this range. Furthermore, if dissociative loss of olefin were taking place to produce $Fe(CO)_4$ and free olefin, parent would be recovered from the reaction of excess CO and the resulting $Fe(CO)_4$. However, no regeneration of parent was observed in these experiments. These observations lead to the conclusion that dissociative loss of olefin is not the main pathway for decomposition of $Fe(CO)_4(C_2Cl_4)$ for CO/C_2Cl_4 pressure ratios above 2.0.

The Fe−CO bond in an olefin iron carbonyl complex is often stronger than the Fe−olefin bond.[8] To our knowledge, dissociative loss of CO has not been previously reported as a primary thermal process in compounds of this type. However, dissociative loss of CO can be described by a modification of eq 8 in which C_2Cl_4 is the adduct (in eqs 5−7 it is CO) and CO is the species lost (in eqs 5−7 it is L). This gives

$$k_{obs} = (k'_d k'_L[L])/(k'_L[L] + k'_{CO}[CO]) \quad (9)$$

From eq 9, for 5 Torr of olefin, a change in k_{obs} from $0.0056k'_d$ to $0.038k'_d$ should be observed in going from 70 to 10 Torr of CO. Therefore, CO dissociation does not explain the independence of k_{obs} on the CO/C_2Cl_4 pressure ratio, in the 2.0−28 range.

In principle, an associative mechanism leading to the disappearance of $Fe(CO)_4(C_2Cl_4)$ is possible. However, such a process should exhibit some pressure dependence, and a relatively high activation energy would be anticipated because the association step would be expected to go through an intermediate with more than 18 electrons.[27]

Because, at high CO/C_2Cl_4 ratios, there is no dependence of k_{obs} on the pressure of CO, C_2Cl_4, or parent, we conclude that a unimolecular process, such as an isomerization, is the most probable transformation leading to the loss of $Fe(CO)_4(C_2Cl_4)$. A number of such transformations are plausible. One is ligand site exchange. The perchloroethylene ligand that is in the equatorial plane of the molecule could exchange with one of the axial CO ligands. However, electronic factors mitigate against this possibility. Olefins donate electrons to the metal center from a π orbital, and such ligands prefer to bond in the equatorial plane of the iron because the metal molecular orbitals that are most favorable for overlap with the electron-donating π orbital(s) are located in this plane.[28] An isomer with an axial perchloroethylene ligand would have an olefin trans to a CO, which will compete with the olefin for back-donation of electrons from the metal. This would be expected to make the equatorial−axial transformation thermodynamically unfavorable. Such differences in stability have been observed for bisethylene complexes of the group VI metals (Cr, Mo, W), in which the complex with two olefins trans to each other is more stable than that with both olefin ligands cis.[29] Furthermore, low-temperature NMR studies on Berry pseudorotations for certain $Fe(CO)_4$(olefin) complexes do not show exchange of an axial CO with an equatorial olefin, meaning that the barrier for such process is relatively high (>30 kcal/mol).[30] Indeed, there are no reports in the literature that we are aware of in which this type of isomerization takes place.

Another possibility is an intramolecular rearrangement in which a chlorine migrates to iron, which can be described as an oxidative addition process.[2,27] Oxidative addition involving reactions of molecular hydrogen, chlorine, bromine, and iodine with iron tetracarbonyl are well-known examples of such process.[23,27] Such a reaction is illustrated in eq 10.

$$Fe(CO)_4 + X_2 \rightarrow Fe(CO)_4(X_2) \rightarrow Fe(CO)_4(X)_2 \ (X = H, Cl, Br, \text{and } I) \quad (10)$$

The oxidative addition of olefins has also been reported. Stoutland and Bergman,[31] as well as Baker and Field,[32] have studied the reaction of ethylene with unsaturated iron, iridium, and rhenium complexes [M]. In all cases, both the η^2-olefin and the vinyl hydride complexes were detected.

$$[M] + H_2C{=}CH_2 \rightarrow [M](\eta^2\text{-}C_2H_4) \quad (11a)$$

$$\rightarrow H[Me](CH{=}CH_2) \quad (11b)$$

Both groups report that the vinyl hydride complex is kinetically favored, but the olefin adduct is thermodynamically more stable. Both studies conclude that, even though both products are the result of the addition of ethylene to the metal center, the two products are produced through different transition states. This implies that the η^2-olefin complex is not an intermediate along the reaction coordinate that leads to the formation of the hydride complex and that, instead, an intermediate involving an agostic metal−hydrogen bond is required. As mentioned in the Introduction, the oxidative addition of chloroethylene ligands to metal complexes is also known; therefore, it is plausible that a reaction (see eq 12) involving the activation of the C−Cl bond could take place in the tetrachloroethylene iron tetracarbonyl complex.

$$Fe(CO)_4 + C_2Cl_4 \rightarrow Fe(CO)_4(C_2Cl_4) \rightarrow ClFe(CO)_4(C_2Cl_3) \quad (12)$$

The activation parameters obtained for the loss of $Fe(CO)_4(C_2Cl_4)$ are $E_a = 21$ kcal/mol and $A = 1 \times 10^{12}$ s^{-1}. The measured A factor is reasonable for a unimolecular process with a tight transition state.[33] Kemmitt and co-workers obtained similar activation parameters for the isomerization of $(PPh_3)_2Pt(C_2Cl_4)$ to $(PPh_3)_2(Cl)Pt(ClC{=}CCl_2)$ in solution.[34]

The major difference between the tetrachloroethylene and the ethylene oxidative addition reactions is that data imply that chloride formation is thermodynamically favored relative to the hydride formation. An estimate of the enthalpy differences between these two oxidative addition processes supports this conclusion. The following thermodynamic cycle can be used to estimate the enthalpy difference for the isomerization of $Fe(CO)_4(C_2Cl_4)$ to $ClFe(CO)_4(C_2Cl_3)$.

$$Fe(CO)_4(C_2Cl_4) \rightarrow Fe(CO)_4 + C_2Cl_4 \quad (13)$$

$$C_2Cl_4 \rightarrow C_2Cl_3 + Cl \quad (14)$$

$$Cl + C_2Cl_3 + Fe(CO)_4 \rightarrow ClFe(CO)_4(C_2Cl_3) \quad (15)$$

From this cycle $\Delta H = -[D(Fe{-}Cl) + D(Fe{-}C_2Cl_3)] + [D(Cl{-}C_2Cl_3) + D(Fe{-}C_2Cl_4)]$. The BDE for a C−Cl bond in tetrachloroethylene is 93 ± 3 kcal/mol.[35] The BDE for perchloroethylene bound to iron tetracarbonyl was calculated[11] using two DFT methods to be between 24 and 30 kcal/mol. The Fe−Cl bond energy is reported as 79 ± 2 kcal/mol,[36] and by scaling the known iridium−ethenyl bond energy,[37] based on a comparison of iridium and iron complexes' BDE's, the iron−vinyl bond can be estimated to be ∼55 kcal/mol. Using these values, the enthalpy for the isomerization is estimated to be −14 ± 12 kcal/mol.

The same cycle can be applied to ethylene: $\Delta H = -[D(Fe{-}H) + D(Fe{-}C_2H_3)] + [D(H{-}C_2H_3) + D(Fe{-}C_2H_4)]$ for the

SCHEME 1

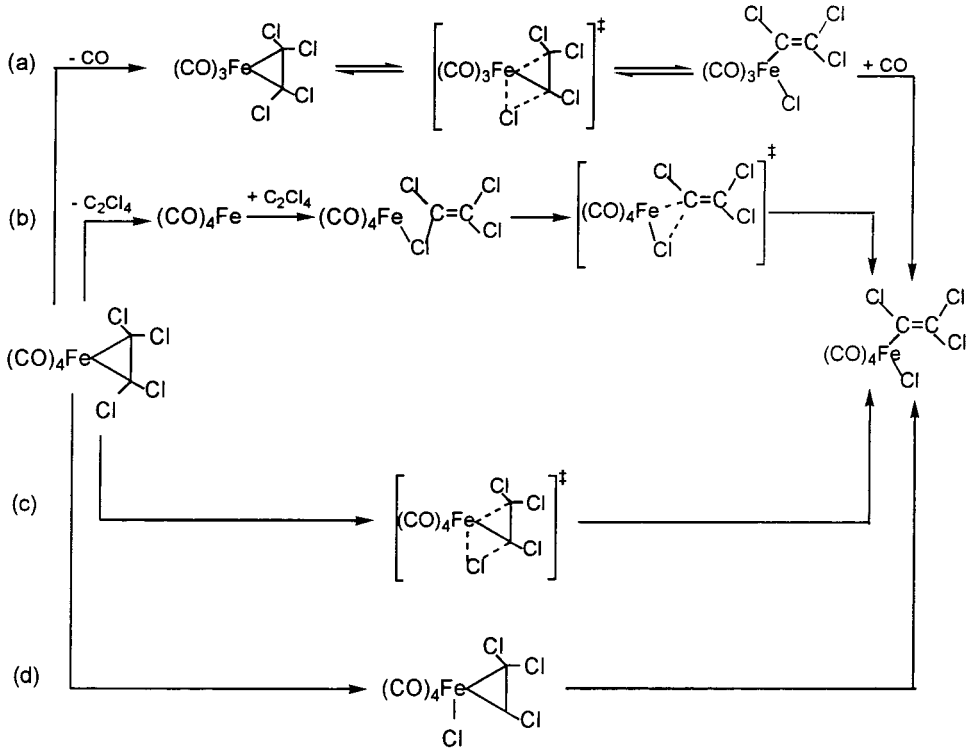

reaction $Fe(DMPE)_2(C_2H_4) \rightarrow HFe(DMPE)_2(C_2H_3)$. Using 62 ± 2 kcal/mol for $D(Fe-H)$,[38] 60 kcal/mol for $D(Fe-C_2H_3)$,[37] 106 ± 3 kcal/mol for $D(H-C_2H_3)$,[31] and 36 ± 4 kcal/mol for $D(Fe-C_2H_4)$,[39] a value of $\Delta H = +20 \pm 12$ kcal/mol is estimated. Even though there are large error brackets and uncertainties in some of the estimated bond energies, the estimate for ΔH for the transformation supports experimental evidence that the isomerization of the monoethylene complex to the hydride is endothermic and that the analogous transformation for the perchloroethylene complex is thermodynamically more favorable. Clearly, the energy necessary to break the iron−ethylene bond added to the energy necessary to break the C−H bond is larger than the sum of the energies for breaking the C−Cl bond and the iron−perchloroethylene bonds. On the other side of the equation, although the formation of a ethenyl−iron bond might be slightly favored over the bonding of the perchloroethenyl moiety to iron, the formation of an Fe−Cl bond is energetically more favorable than the formation of an Fe−H bond. It should also be mentioned that, as shown by Wrighton and co-workers in their matrix experiments, although the addition of C_2H_4 to $Fe(DMPE)_2$ yields $HFe(DMPE)_2(C_2H_3)$, there is no evidence that the same process takes place on the addition of C_2H_4 to $Fe(CO)_4$.[40]

The facts that the isomerization of $Fe(CO)_4(C_2Cl_4)$ takes place with a barrier of 21 kcal/mol and that there is no evidence of olefin dissociation imply that the barrier for olefin dissociation is above the barrier for isomerization, particularly because a dissociative process would be expected to have a larger preexponential factor than that measured for the isomerization pathway. Because there is no observed temperature dependence for the rate constant for addition of a C_2Cl_4 ligand to $Fe(CO)_4$, the activation energy for the dissociative loss of C_2Cl_4 can be directly related to the bond enthalpy.[41] Even though these measurements are made in the presence of olefin, one of the olefin/CO ratios that was employed was such that $k_{obs} = 0.87k_d$. Thus, the BDE for the iron−perchloroethylene bond in $Fe(CO)_4(C_2Cl_4)$ is expected to be greater than ∼21 kcal/mol. Prior DFT calculations support such a conclusion regarding the magnitude of the BDE for $Fe(CO)_4(C_2Cl_4)$.[11]

For CO/C_2Cl_4 ratios below 2 and temperatures below 304 K, the decay of $Fe(CO)_4(C_2Cl_4)$ becomes biexponential. The experimental data do not show evidence of a strong dependence of the decay rates on the CO/C_2Cl_4 ratio, although the error brackets in the determination of the rates are large, especially for the rate of the fast component. On the basis of a proposed global mechanism, which will be discussed in section IV.G, the fast decay should have a weak dependence on the CO/C_2Cl_4 ratio under these experimental conditions. However, the predicted change in the rates are of the order of the experimental error. Also, the fast decay could be associated with establishment of a preequilibrium involving $Fe(CO)_4(C_2Cl_4)$ and $Fe(CO)_3(C_2Cl_4)_2$, prior to the isomerization reaction (slow component), which is the rate-limiting decomposition path.

B. Mechanism for the Thermal Isomerization of $Fe(CO)_4(C_2Cl_4)$. *A priori* there are at least four obvious possible mechanisms for the thermal isomerization of the monoolefin complex (see Scheme 1, a−d). Mechanisms a and b, which involve ligand dissociation, can be ruled out on the basis of the fact that the isomerization rate does not depend on ligand or CO pressure. Note that mechanism b is intended as a generic mechanism for a stepwise rearrangement of the initial monoolefin complex. The formation of a 19-electron complex, as in d, involves the placement of an electron in an antibonding metal orbital, which is energetically unfavorable. Although a 19-electron intermediate resulting from the transfer of a chlorine prior to the formation of the iron−vinyl bond is possible, it would be quite surprising if the activation barrier for formation of such a species were not larger than the measured value of ∼21 kcal/mol. Thus, mechanism c, involving concerted chorine atom transfer and iron vinyl bond formation in a "metallocycle-like" transition state seems most likely. In fact, an analogous metallocycle intermediate has been proposed by Stoutland and Bergman to explain the isomerization of $HIr(\eta^5\text{-Cp})(PMe_3)(C_2H_3)$ to its $(\eta^5\text{-Cp})(PMe_3)Ir(\eta^2\text{-}C_2H_4)$ isomer.[31]

Note that formation of a metallocycle transition state involves a change in the binding of the olefin at the iron center from a configuration involving coordination of ligand π electrons to one involving two Fe−C σ bonds. Indeed, the bonding of haloalkenes in metal complexes seems to have some metallocycle character rather than pure coordination through the double bond.[2,15] Strongly electron-withdrawing substituents around the double bond increase the propensity for back-donation of electron density. In such complexes, back-donation is more important if the metal is relatively electron rich, as is iron(0). Because back electron donation involves the π^* antibonding orbital of the olefin, the bond order of the C═C bond decreases and attains more of a single-bond character. The result is elongation of the carbon−carbon bond and bending of the substituents away from the metal, as the carbon atoms have more sp^3 character. This effect has been confirmed by gas-phase electron diffraction structures of $Fe(CO)_4(C_2H_4)$ and $Fe(CO)_4(C_2F_4)$.[42,43] DFT calculations predict the same behavior in the tetrachloroethylene complex.[11] Although there are no experimental geometrical parameters for $Fe(CO)_4(C_2Cl_4)$, DFT results for the geometry of $Fe(CO)_4(C_2Cl_4)$ more closely resemble the geometry of $Fe(CO)_4(C_2F_4)$ than that of $Fe(CO)_4(C_2H_4)$.[11] This is consistent with a concerted oxidative addition process involving the formation of a metallocycle-like transition state being more favorable in the perchloroethylene complex than in the analogous ethylene complex.

C. Formation and Decay of $ClFe(CO)_4(C_2Cl_3)$. As discussed in the Results section and shown in Figure 5b, when a mixture of ∼50 mTorr of $Fe(CO)_5$, ∼5 Torr of C_2Cl_4, and more than 10 Torr of CO is photolyzed, a new set of bands (2089, 2109, and 2166 cm^{-1}) grows in during photolysis. These bands are assigned to species **IV**, which is sufficiently stable that the bands can be observed in FTIR spectra. The blue shifting of the absorptions of species **IV** with respect to absorptions of the monoolefin complex is consistent with species **IV** being $ClFe(CO)_4(C_2Cl_3)$. A mechanism to explain the growth of $ClFe(CO)_4(C_2Cl_3)$ during photolysis and its dependence on CO pressure is shown in eqs 16−19.

Photolysis of $Fe(CO)_4(C_2Cl_4)$ can lead to loss of CO to produce $Fe(CO)_3(C_2Cl_4)$. This is followed by the oxidative addition of C_2Cl_4 to yield a 16-electron chloride vinyl complex, which can then add CO to form the 18-electron perchlorovinyl iron tetracarbonyl chloride complex.

$$Fe(CO)_4 + C_2Cl_4 \rightarrow Fe(CO)_4(C_2Cl_4) \quad (16)$$

$$Fe(CO)_4(C_2Cl_4) \overset{h\nu}{\rightleftharpoons} Fe(CO)_3(C_2Cl_4) + CO \quad (17)$$

$$Fe(CO)_3(C_2Cl_4) \rightleftharpoons ClFe(CO)_3(C_2Cl_3) \quad (18)$$

$$ClFe(CO)_3(C_2Cl_3) + CO \rightleftharpoons ClFe(CO)_4(C_2Cl_3) \quad (19)$$

The increase in the peak absorbance of the $ClFe(CO)_4(C_2Cl_3)$ absorption bands with increasing photolysis time is consistent with this mechanism. At a CO pressure of 10 Torr the ratio of the peak of the absorption band of the monoolefin to that of the chloride product decreased from 19:2 after 150 shots to 8:2 after 300 shots. When the CO pressure is 70 Torr, the monoolefin-to-chloride ratio does not change significantly after ∼1 min of photolysis at 5 Hz, suggesting that a photostationary state is reached in the presence of a large excess of CO. With enough CO present, $ClFe(CO)_3(C_2Cl_3)$ can be trapped as $ClFe(CO)_4(C_2Cl_3)$ before it has a chance to revert to $Fe(CO)_3(C_2Cl_4)$. Thus, the rate of growth of $ClFe(CO)_4(C_2Cl_3)$ increases as more CO is added in the 10−35 Torr pressure range. Additional evidence for the photolytic growth of the chloride comes from an analysis of FTIR spectra taken during photolysis. In a manner consistent with the proposed mechanism the growth of the perchlorovinyl iron tetracarbonyl chloride product exhibits an induction time; that is, it only starts growing after some $Fe(CO)_4(C_2Cl_4)$ has been formed. Further evidence for the mechanism in eqs 16−19 comes from diode laser experiments at 2089 and 2109 cm^{-1}. In these experiments perchlorovinyl iron tetracarbonyl chloride was observed to grow as a result of photolysis only when the CO pressure exceeded ∼10 Torr, and the intensity of the signal increased with increasing CO pressure. Although photolytic loss of olefin rather than CO seems more typical in the metal−olefin complexes that have been studied, the mechanism in eqs 16−19 only requires that CO loss is a nonnegligible photolytic pathway.[26,29,40,44]

Baker and Field[32] reported that photolysis of $Fe(DMPE)_2(C_2H_4)$ yields the vinyl $Fe(DMPE)_2$ hydride complex $HFe(DMPE)_2(C_2H_3)$, but they did not present a mechanism for its formation. We hypothesize that formation of this hydride complex is likely to involve breaking of the Fe−olefin bond and subsequent formation of an intermediate with an agostic H−Fe bond.

$ClFe(CO)_3(C_2Cl_4)$ decays in about 10 min at room temperature, with no measurable dependence on ligand pressure. The Arrhenius parameters for its disappearance are $E_a = 7$ kcal/mol and $A = 10^3$ s^{-1}. The very small preexponential factor virtually precludes a direct elementary dissociative step leading to decay of $ClFe(CO)_4(C_2Cl_4)$. These parameters suggest that the disappearance of this product involves a heterogeneous pathway and/or a complex decomposition process for which the observed rate constant is actually a phenomenological rate constant that is potentially the quotient and/or product of microscopic rate constants. Such a process can be represented generically in eqs 20−22.

$$ClFe(CO)_4(C_2Cl_4) \underset{k_2}{\overset{k_1}{\rightleftharpoons}} ClFe(CO)_3(C_2Cl_4) + CO \quad (20)$$

$$ClFe(CO)_4(C_2Cl_4) \xrightarrow{k_p} \text{wall reactions and other processes} \quad (21)$$

$$ClFe(CO)_3(C_2Cl_4) \xrightarrow{k_o} \text{other products} \quad (22)$$

This mechanism yields a k_{obs} that is equal to $(k_p k_2[CO] + k_1 k_o)/(k_2[CO])$.

Note that, if CO dissociation were considered (eq 20), there would be a CO-dependent equilibrium involved in the kinetics. However, the accuracy with which the decay rates can be determined for $ClFe(CO)_3(C_2Cl_4)$ degrades at low CO pressures because of the limited signal-to-noise ratio at these pressures. For larger CO pressures, for which the rate can be measured more accurately, there is no evidence of a CO dependence. However, this is not incompatible with the mechanism indicated above. At high CO pressure, the equilibrium in eq 20 is displaced to the left, and therefore, the dominant decomposition path is the reaction of the product on the cell walls. When the CO pressure is sufficiently high that $k_p k_2[CO] \gg k_1 k_o$, the observed rate constant would then be equal to the decay rate for wall reactions and/or other decay processes. Under these conditions, the preexponential factor could be for wall reactions, or it could be a phenomenological preexponential factor resulting from a weighted sum of decay channels. The decay products could remain on the cell walls or precipitate out of the gas phase, explaining why we do not directly observe decomposition products in the gas phase.

D. Oxidative Addition in the 16-Electron Complex: $Fe(CO)_3(C_2Cl_4)$. Equations 16−19 provide a mechanism for the formation of $ClFe(CO)_4(C_2Cl_4)$ as a result of photolysis of $Fe(CO)_4(C_2Cl_4)$ and explain the lack of an observable dependence on the pressure of CO present in the reaction mixture. This mechanism implies that the oxidative addition of the C_2Cl_4 ligand that occurs in the 16-electron $Fe(CO)_3(C_2Cl_4)$ complex to form $ClFe(CO)_3(C_2Cl_3)$ is considerably more facile than the corresponding process in $Fe(CO)_4(C_2Cl_4)$. A more facile oxidative addition reaction in $Fe(CO)_3(C_2Cl_4)$ relative to $Fe(CO)_4(C_2Cl_4)$ is certainly plausible considering that the open coordination site in the 16-electron species could facilitate the formation of an agostic chlorine−iron bond, which is necessary for the proposed transition state.

Oxidative addition in 16-electron iron−olefin complexes has been observed before, with the β-atom transfer process having been studied in the most detail.[1,2,27,45] For example, $Fe(CO)_3(\eta^2\text{-}C_3H_6)$ reacts to form the allyl hydride complex $HFe(CO)_3(\eta^3\text{-}C_3H_5)$. The gas-phase reaction is very fast ($>10^{10}$ s^{-1}) and probably unactivated (<3.5 kcal/mol).[46] Similarly, the photolysis of $Fe(CO)_5$ with $CH_2{=}CH{-}CH_2Cl$ in pentane yields a relatively stable allyl iron chloride complex, $ClFe(CO)_3(\eta^3\text{-}C_3H_5)$.[47] α-atom transfer reactions, as part of oxidative addition processes, have also been reported in 16-electron complexes.[12,34,48] The oxidative addition reaction in the $(PPh_3)_2Pt(C_2Cl_4)$ complex to form $(PPh_3)_2ClPt(C_2Cl_3)$ is one example.[34] Another example is the conversion of $(\eta^2\text{-}HBPf_3)Ir(CO)(\eta^2\text{-}C_2H_4)$ to its vinyl hydride isomer as a result of the oxidative addition of C_2H_4.[48]

In the absence of added CO, the decay of $Fe(CO)_3(C_2Cl_4)$ is governed by the rate law for the following processes:

$$Fe(CO)_3(C_2Cl_4) \underset{k_r}{\overset{k_f}{\rightleftharpoons}} ClFe(CO)_3(C_2Cl_3) \quad (K_{eq} = k_f/k_r) \qquad (23)$$

$$Fe(CO)_3(C_2Cl_4) + C_2Cl_4 \xrightarrow{k_+} Fe(CO)_3(C_2Cl_4)_2 \qquad (24)$$

The value of K_{eq} determines which of two rate expressions are observed. If $k_f \gg k_r$, the chloride isomer is favored, and the rate of rise of the bisolefin is given by[46]

$$k_{obs} = k_r k_+ [C_2Cl_4]/(k_f + k_+[C_2Cl_4]) \qquad (25)$$

Assuming that the isomerization is faster than the addition of a second olefin, that is, $k_f \gg k_+[C_2Cl_4]$, then k_{obs} is approximately equal to $k_+[C_2Cl_4]/K_{eq}$. The rise of bisolefin product would be dependent on the pressure of olefin, as is observed. However, the implication of this expression is that, when the rate of rise of olefin is plotted against the olefin pressure, the slope should be equal to the addition rate constant (k_+) divided by the equilibrium constant for eq 23. On the other hand, if $k_r \gg k_f$, the monoolefin is favored, and the observed rate for the rise of product is simply

$$k_{obs} = k_+[C_2Cl_4] \qquad (26)$$

and the slope of the rate of rise of product versus olefin pressure is simply the addition rate constant. As will be discussed in section IV.E, the rate constant for addition of a second tetrachloroethylene ligand to $Fe(CO)_3(C_2Cl_4)$ seems to be "abnormally" low when it is compared to the rate constants for addition of other olefins to analogous unsaturated $Fe(CO)_3(C_2X_4)$ complexes. This observation could imply that what has been measured is k_+/K_{eq}, and not simply k_+. This would further imply that species **I** is the chloride, rather than the monoolefin. However, if the measured rate is the addition rate constant divided by the equilibrium constant, then a change in temperature would be expected to lead to a change in the observed rate. As a general rule, the rate constants for addition of olefins to unsaturated metal carbonyls are temperature-independent[10,46] however, as long as ΔG is not zero, there should be a temperature dependence to the equilibrium constant. As mentioned previously, within the experimental error, the rate constant for formation of $ClFe(CO)_4(C_2Cl_3)$ is independent of temperature. This temperature independence implies that the equilibrium favors the monoolefin and that the observed intermediate **I** is the unsaturated monoolefin carbonyl, $Fe(CO)_3(C_2Cl_4)$. Additional evidence to support this conclusion is found in the FTIR spectra of samples containing very low CO pressures. In the presence of a small amount of CO, both species in the equilibrium in eq 23 will compete for CO. If $ClFe(CO)_3(C_2Cl_3)$ is favored by the equilibrium, then $ClFe(CO)_4(C_2Cl_3)$ should be the main CO addition product. However, spectra of a mixture containing 0.5 Torr of CO revealed mostly $Fe(CO)_4(C_2Cl_4)$, which is formed as a result of the addition of CO to $Fe(CO)_3(C_2Cl_4)$. It should also be noted that once species **I** is assigned as $Fe(CO)_3(C_2Cl_4)$, it is clear that species **II** is $Fe(CO)_3(C_2Cl_4)_2$.

With a large quantity of CO present, the dominant pathway for production of monoolefin is addition of C_2Cl_4 to $Fe(CO)_4$, and as shown previously, the dominant channel for production of $ClFe(CO)_4(C_2Cl_3)$ is via photolysis of $Fe(CO)_4(C_2Cl_4)$. When high pressures of CO are present, the unsaturated chloride complex $[ClFe(CO)_3(C_2Cl_3)]$ can be trapped as $ClFe(CO)_4(C_2Cl_3)$. Although $ClFe(CO)_3(C_2Cl_3)$ can isomerize to $Fe(CO)_3(C_2Cl_4)$, this latter species could add CO to produce $Fe(CO)_4(C_2Cl_4)$, which could then be photolyzed, lose CO to produce a 16-electron species, which could then isomerize. This cycle is repeated with each photolysis pulse, providing a means for $ClFe(CO)_4(C_2Cl_3)$ to accumulate.

The results discussed above on the formation of the unsaturated chloride, $ClFe(CO)_3(C_2Cl_3)$, from the 16-electron monoolefin, $Fe(CO)_3(C_2Cl_4)$, imply that this oxidative addition process must be rapid enough to compete with the addition of CO to $Fe(CO)_3(C_2Cl_4)$ to re-form $Fe(CO)_4(C_2Cl_4)$. Thus, it is clear that isomerization is faster than the addition of ligand, placing the rate of isomerization as $>6 \times 10^6$ s^{-1}. An estimate of the rate for the reverse reaction in eq 23 can be made from the relative yields of $Fe(CO)_4(C_2Cl_4)$ and $ClFe(CO)_4(C_2Cl_3)$ after photolysis. Assuming that the rate for addition of CO to $ClFe(CO)_3(C_2Cl_3)$ is in the 10^{-11}−10^{-12} cm^3 molecule^{-1} s^{-1} range, a simple photolytic model predicts that in order to obtain the experimentally observed relative yields, the rate for the reverse reaction must be on the order of 10^9 s^{-1}, using a value for k_f in eq 23 of 6×10^6 s^{-1}.

E. Addition Rate Constants. Table 1 contains the rate constants for the additions of C_2H_4, C_2F_4, and C_2Cl_4 to $Fe(CO)_3$, $Fe(CO)_4$, and $Fe(CO)_3$(olefin). Available data indicate that, in general, the rate constant for addition of a ligand to $Fe(CO)_3$ is $\sim 10^2$ times faster than the corresponding rate constant for addition to $Fe(CO)_4$.[49] $Fe(CO)_3$ has been predicted to have a triplet ground state, and thus, addition of a ligand (L′) to form a triplet $Fe(CO)_3L'$ complex is expected to be spin-conserving.[8,50] Because $Fe(CO)_4$ has been reported to have a triplet ground state[51] and available evidence indicates that, at least for weakly bound ligands, $Fe(CO)_3L'$ complexes have triplet ground states,[49] addition of a singlet ground-state ligand to $Fe(CO)_4$ requires a spin change. This necessity for an intersystem-crossing process, which involves accessing a restricted region of phase space, leads to a relatively small addition rate constant compared to the rate constant for the addition of the corre-

TABLE 1: Rate Constants[a] for Addition of Some Olefins to Unsaturated Iron Carbonyls

	L = C_2H_4[b]	L = C_2F_4[b]	L = C_2Cl_4[c]
$Fe(CO)_3 + L$	$(22 \pm 2) \times 10^{-11}$	$(3.3 \pm 1.2) \times 10^{-11}$	$(3.0 \pm 0.8) \times 10^{-11}$
$Fe(CO)_4 + L$	$(1.7 \pm 0.2) \times 10^{-13}$	$(0.18 \pm 0.05) \times 10^{-13}$	$(1.2 \pm 0.3) \times 10^{-13}$
$Fe(CO)_3L + L$	$(11 \pm 3) \times 10^{-12}$	$(5.4 \pm 1.7) \times 10^{-12}$	$(0.19 \pm 0.04) \times 10^{-12}$
$Fe(CO)_3L + CO$	$(4.3 \pm 0.7) \times 10^{-12}$	−	$(2.4 \pm 0.6) \times 10^{-12}$

[a] Rate constants are in cm^3 $molecule^{-1}$ s^{-1}. [b] From refs 10 and 49. [c] This work

sponding ligand to $Fe(CO)_3$, for which this constraint is not expected to be operative. Larger rate constants for addition of a ligand, L, have generally been observed when one CO is replaced by another ligand (L′) to produce an $Fe(CO)_3L'$ species. Possible reasons for this are discussed in ref 49.

The rate constants for the addition of C_2Cl_4 to unsaturated iron carbonyls follow the general trend outlined above. The rate constant for addition of C_2Cl_4 to $Fe(CO)_3$ is 250 times larger than the rate constant for its addition to $Fe(CO)_4$. Replacing a CO ligand by tetrachloroethylene increases the rate constant for C_2Cl_4 addition, although not by much. The rate constant for addition of C_2Cl_4 to $Fe(CO)_3(C_2Cl_4)$ is only 1.6 times larger than the rate constant for its addition to $Fe(CO)_4$. Also, the rate constant for addition of C_2Cl_4 to $Fe(CO)_3(C_2Cl_4)$ is small relative to the rate constants for the addition of ethylene and tetrafluoroethylene to their respective olefin tricarbonyl iron complexes. The relatively small rate constant for the addition of a second C_2Cl_4 ligand could be the result of steric factors. The binding of a second olefin is preferred in the equatorial plane of the molecule.[28] Thus, there could be greater steric hindrance in its approach to the $Fe(CO)_3(C_2X_4)$ moiety if the olefin has large substituents around the double bond. This picture is consistent with the relative magnitudes of the rate constants for addition of CO and C_2Cl_4 to $Fe(CO)_3(C_2Cl_4)$, for which the former is ~12 times larger than the latter. Molecular mechanics calculations using the Tripos force field, available in the Sybyl molecular mechanics program,[52] were employed to qualitatively compare the effect of the substituent around the double bond on the steric repulsive term of the van der Waals energy when a C_2X_4 ligand approaches an unsaturated $Fe(CO)_3(C_2X_4)$ fragment. In all cases, the approaching olefin was the same as the bound olefin. The steric repulsive contribution to the overall energy is much larger for tetrachloroethylene than for both ethylene and tetrafluoroethylene. To minimize the repulsive interaction, the incoming ligand must rotate slightly so that the incoming olefin is not parallel to the bound ligand. At the same time, the iron carbonyl fragment, which was assumed to be of C_{2v} symmetry,[44] must deform by bending the axial carbonyl ligands away from the incoming ligand.

The rate constant for addition of tetrachloroethylene to $Fe(CO)_4$ is slightly smaller than that for the corresponding process for ethylene but larger than that for perfluoroethylene. Interestingly, these results follow the pattern associated with changes in electron-donating character of the incoming ligand: C_2H_4 is a better electron donor than C_2Cl_4, and C_2Cl_4 is better than C_2F_4. The electron-donating character of the olefin could affect the rate constant if it leads to a longer-lived complex on the triplet potential energy surface.[49]

The rate of formation of a polynuclear complex from the reaction of $Fe(CO)_5$ with $Fe(CO)_3(C_2Cl_4)$ is equal to $(9.7 \pm 3.5) \times 10^{-12}$ cm^3 $molecule^{-1}$ s^{-1} at 24 °C. Although there is no definitive evidence as to the nature of this complex, prior studies[22,53] indicate that such reactions are typically association processes, which, in this case, would lead to formation of $Fe_2(CO)_8(C_2Cl_4)$. The rate constant for the reaction of $Fe(CO)_5$ with $Fe(CO)_3(C_2Cl_4)$ is very similar in magnitude to the rate constant for the addition of $Fe(CO)_5$ to $Fe(CO)_3(C_2H_4)$, which is equal to $(4 \pm 2) \times 10^{-11}$ cm^3 $molecule^{-1}$ s^{-1} at 24 °C.[8] As pointed out by Ryther and Weitz,[53] the rearrangements necessary to produce products in some polynuclear-species-forming reactions do not have a major influence on the rate constants for these processes. This was attributed to the fact that, on complexation, the energy released into the internal degrees of freedom of the association complex can facilitate the geometrical rearrangement required to produce a stable species. Although the rate constant for addition of perchloroethylene to $Fe_2(CO)_8$ is much smaller, $(4.4 \pm 2.5) \times 10^{-14}$ cm^3 $molecule^{-1}$ s^{-1} at 24 °C, than the rate constant for reaction of $Fe(CO)_5$ with $Fe(CO)_3(C_2Cl_4)$, it is ~6 times larger than the rate constant reported by Ryther and Weitz[53] for the addition of CO to $Fe_2(CO)_8$. This difference in magnitude for perchloethylene and CO reacting with $Fe_2(CO)_8$ is comparable to that observed for the rates of addition of C_2Cl_4 and CO to $Fe(CO)_4$.

TABLE 2: Carbonyl Stretch IR Absorptions for Some Olefin Iron Carbonyl Complexes

species	conditions[h] (K)	frequency (cm^{-1})[i]
$Fe(CO)_4(C_2H_4)$[a]	gas (298)	2095 (0.11), 2024 (0.74), 2020 (1.00), 2007 (0.50), 2002 (0.75)
$Fe(CO)_4(C_2F_4)$[b]	gas (297)	2135 (0.04), 2074 (1.00), 2043 (0.78)
$Fe(CO)_4(C_2Cl_4)$[c]	gas (297)	2125 (0.45), 2069 (1.00), 2039 (0.73)
$Fe(CO)_4(C_2Cl_4)$[d]	hex (298)	2134 (s), 2072 (vs), 2040 (s), 2004 (w)
$Fe(CO)_4(C_2Cl_2F_2)$[e]	hex (298)	2126 (m), 2063 (s) 2032 (s)
$Fe(CO)_3(C_2H_4)_2$[a]	gas (298)	2069 (0.07), 2001 (0.80), 1997 (1.00)
$Fe(CO)_3(C_2F_4)_2$[b]	gas (297)	2147 (0.08), 2091(1.00), 2068 (0.60)
$Fe(CO)_3(C_2Cl_4)_2$[c]	gas (297)	2084 (1.0), 2057 (0.4)
$Fe(CO)_3(C_2H_4)$[f]	MCH (90)	2041 (0.6), 1963 (0.8), 1957 (1.0)
$Fe(CO)_3(C_2Cl_4)$[c]	gas (297)	2076
$ClFe(CO)_4(C_2Cl_3)$[c]	gas (297)	2166 (0.2), 2109 (1.0), 2089 (0.8)
$ClFe(CO)_4Cl$[g]	TCE (298)	2164 (0.19), 2124 (1.00), 2108 (0.77), 2084 (0.85)

[a] Weller, B. H.; Miller, M. E.; Grant, E. R. *J. Am. Chem. Soc.* **1987**, *109*, 352. [b] House, P. G.; Weitz, E. *J. Phys. Chem. A* **1997**, *101*, 2988. [c] This work. [d] Fields, R.; Godwin, G. L.; Haszeldine, R. N. *J. Organomet. Chem.* **1971**, *26*, C70. [e] Fields, R.; Germain, M. M.; Haszeldine, R. N.; Wiggans, P. W. *J. Chem. Soc. A* **1970**, 1969. [f] Wuu, Y.; Bentsen, J. G.; Brinkley, C. G.; Wrighton, M. S. *Inorg. Chem.* **1987**, *26*, 530. [g] Noack, K. *Helv. Chim Acta* **1962**, *45*, 1847. [h] gas = gas phase, hex = hexanes solution, MCH = methylcyclohexane matrix, and TCE = tetrachloroethylene solution. [i] Relative intensities in parentheses.

F. Carbonyl Stretching Frequencies. Table 2 lists the carbonyl stretching frequencies for the species detected in this work, along with relevant frequencies for related olefin iron carbonyl complexes. A comparison of the frequencies for the monoolefin tetracarbonyl complexes reveals that, as expected, the halogenated olefin ligands shift the carbonyl absorptions toward higher frequency with respect to those of ethylene because the halogen substituents on the olefin make these molecules more electron-withdrawing than ethylene. Electron-withdrawing ligands remove electron density from the metal, making it less available for back-bonding to the carbonyl ligands. As a consequence of this the Fe−CO bond distance increases, while the C−O bond distance decreases, generally leading to a shift in the CO stretching mode(s) to higher

SCHEME 2

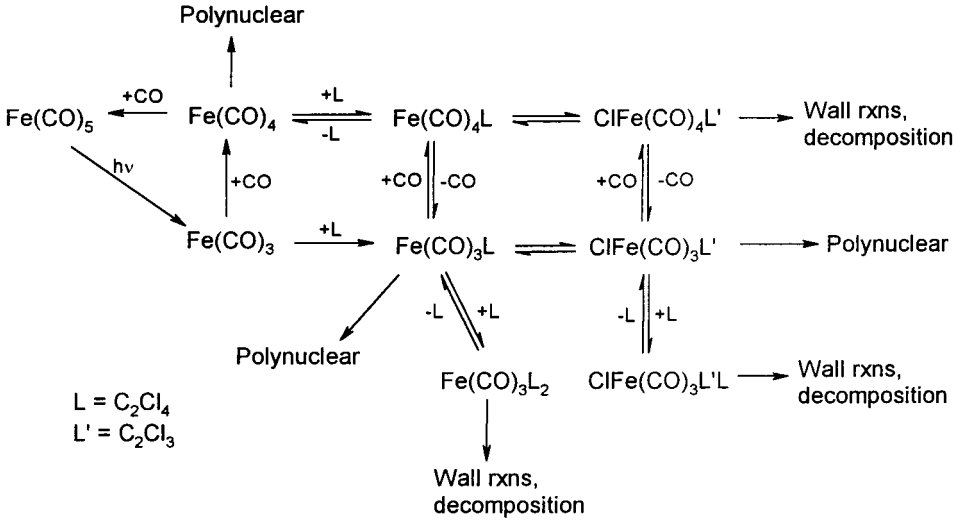

frequency. DFT calculations[11] of bond distances are consistent with results from electron diffraction studies,[42,43] both of which support this picture. In a manner consistent with this picture the absorptions bands of the tetrafluoroethylene complex are slightly blue-shifted relative to those of the tetrachloroethylene complex as a result of the stronger electron-withdrawing effect of the fluorine atoms as compared to that of the chlorine atoms.

The same trend is observed for the bisolefins. The relative intensities and the frequency separation of the bands that were detected support the correspondence of the 2084 and 2057 cm^{-1} bands of the bistetrachloroethylene complex with the 2091 and 2068 cm^{-1} bands in its tetrafluoroethylene analogue. On the basis of the bistetrafluoroethylene spectra, an absorption for the bistetrachloroethylene at a still higher energy would be predicted. However, the range of operation of the diode laser used in these experiments precluded operation in the region where this absorption would be expected (near 2140 $cm^{-1.}$)

A comparison of the shifts in the absorption of the bisolefin complexes relative to those in their monoolefin analogues can be made with the assumption that both the mono- and bisolefin complexes have C_{2v} symmetry.[26] For ethylene, the bisolefin absorptions are red-shifted with respect to the corresponding monoolefin absorptions. However, in the case of the bis halogenated olefin complexes, they are blue-shifted, with a larger blue shift for the fluorine relative to the chlorine-containing complex. The addition of an electron-withdrawing ligand leads to a decrease in the electron density available for back-bonding. This weakens the Fe−CO bond and leads to a stronger CO bond relative to the monoolefin. However, when bound to an iron tetra- or tricarbonyl, ethylene is a better electron donor than electron acceptor.[2] An extra ethylene leads to more electron density around the metal which is then available for back-donation to the carbonyl, decreasing the Fe−CO bond distance and elongating the CO bond.

Through analogous reasoning, a perchlorovinyl chloride is expected to withdraw more electron density than an olefin. The positions of the iron tetracarbonyl dichloride absorption bands support this expectation. Thus, a chloride perchlorovinyl tetracarbonyl complex should have CO absorptions bands that are blue-shifted with respect to the monoolefin and bisolefin complexes, as is the case for the monochloride species reported in this work.

G. Overall Mechanism for Addition of Perchloroethylene to Unsaturated Iron Carbonyls and Kinetics Simulations. A mechanism that is consistent with all of the observations discussed in this work is shown in Scheme 2. Photolysis of $Fe(CO)_5$ at 308 nm generates $Fe(CO)_3$ which can add either CO or C_2Cl_4 or both. At low CO pressures, the initial formation of $Fe(CO)_3(C_2Cl_4)$ is favored (Figure 1). $Fe(CO)_3(C_2Cl_4)$ can undergo an oxidative addition reaction to form $ClFe(CO)_3(C_2Cl_3)$. This process is reversible and an equilibrium is established between these species (eq 23). Although C_2Cl_4 can add to either of these species, the bisolefin, $Fe(CO)_3(C_2Cl_4)_2$, is the primary product, as the equilibrium between $Fe(CO)_3(C_2Cl_4)$ and $ClFe(CO)_3(C_2Cl_3)$ significantly favors the 16-electron monoolefin complex. The bisolefin lives for longer than 500 ms, but it was difficult to detect this species using FTIR spectroscopy or the diode laser. The optimum conditions for observing the bisolefin with either the FTIR or the diode laser were those in which the pressure of CO were minimal (<1 Torr). However, even under those conditions, the limited signal-to-noise levels of the bisolefin signals makes the analysis of the bisolefin behavior difficult and is consistent with the species being present at low concentration.

Under conditions such that the CO/C_2Cl_4 pressure ratio is high, the addition of CO to $Fe(CO)_3$ to yield $Fe(CO)_4$ is the dominant initial process. Addition of olefin to $Fe(CO)_4$ produces $Fe(CO)_4(C_2Cl_4)$, which when photolyzed can produce $ClFe(CO)_4(C_2Cl_3)$ via addition of CO to $ClFe(CO)_3(C_2Cl_3)$, which is present because of the $Fe(CO)_3(C_2Cl_4)-ClFe(CO)_3(C_2Cl_3)$ equilibrium. Because this equilibrium favors $Fe(CO)_3(C_2Cl_4)$, $ClFe(CO)_3(C_2Cl_3)$ is not directly observed but, rather, serves as an intermediate in the generation of $ClFe(CO)_4(C_2Cl_3)$. In principle, olefin could also add to $ClFe(CO)_3(C_2Cl_3)$. However, we found no evidence for the anticipated $ClFe(CO)_3(C_2Cl_3)(C_2Cl_4)$ product. This could be for a number of reasons. For example, $ClFe(CO)_3(C_2Cl_3)(C_2Cl_4)$ could very unstable to ligand loss and/or rearrangement and/or it could be very photolabile with respect to 308-nm radiation. Additionally, the C_2Cl_4 pressure was limited to ~5 Torr, so even if it forms, it would be expected to be present at low concentration.

As discussed in section III.B, the absorptions observed for species **III** match up very well with those reported by Haszeldine and co-workers for a compound they identified as $Fe(CO)_4(C_2Cl_4)$.[16] However, because there has been no determination of the structure of this compound, it is, at least in principle, possible that this compound is actually $ClFe(CO)_4(C_2Cl_3)$. In this case, species **IV** would be $Fe(CO)_4(C_2Cl_4)$. However, this

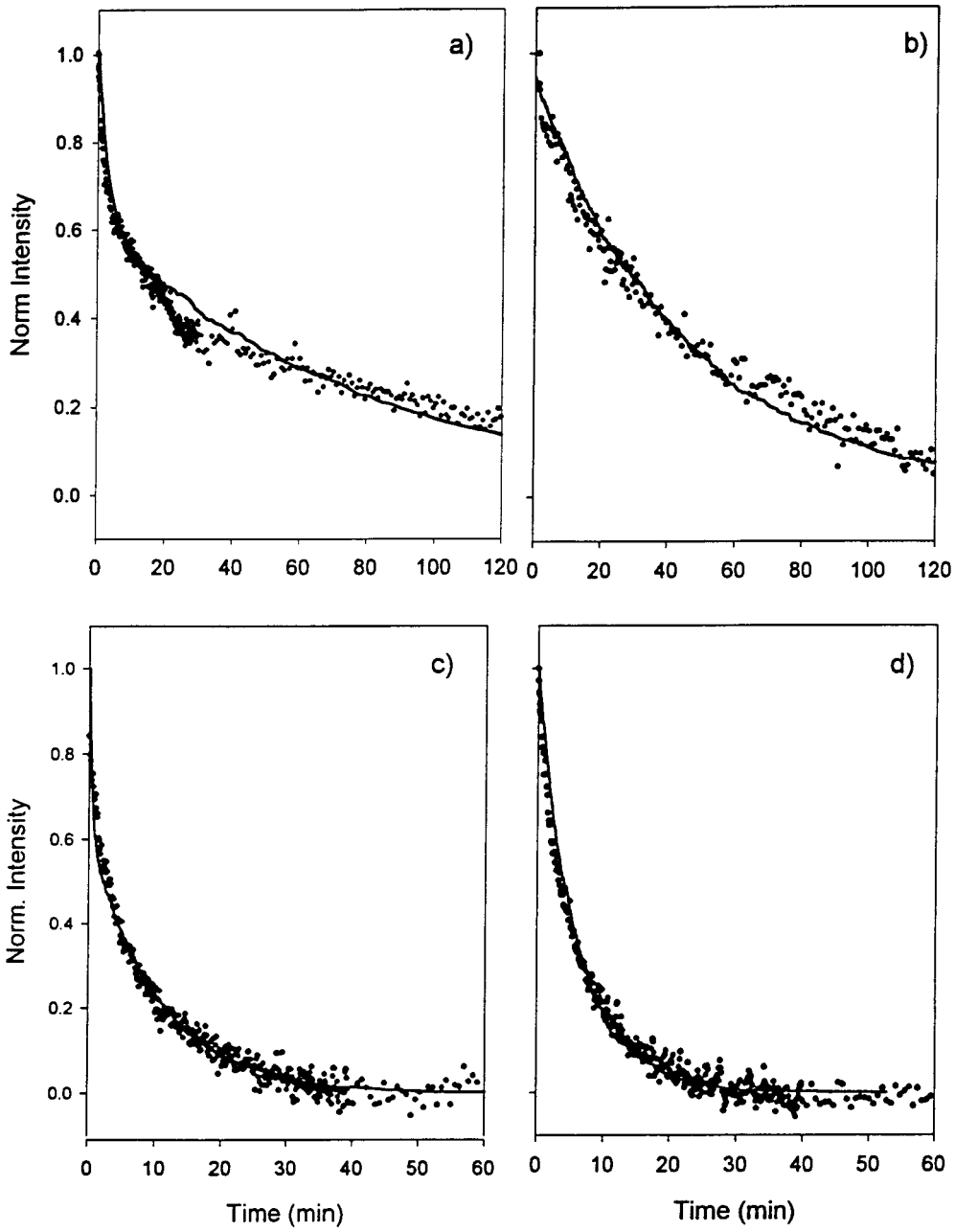

Figure 8. Plots of experimentally obtained signals for the loss of $Fe(CO)_4(C_2Cl_4)$ (solid circles) that are compared to simulations (solid lines) based on Scheme 2: (a) 297 K and $CO/C_2Cl_4 = 0.5$, (b) 297 K and $CO/C_2Cl_4 = 14$, (c) 315 K and $CO/C_2Cl_4 = 0.5$, and (d) 315 K and $CO/C_2Cl_4 = 14$. In each case, the olefin pressure was 5 Torr.

possibility can be excluded on the basis of the kinetics observed in the present study. For species **III** to be $ClFe(CO)_4(C_2Cl_3)$, it would have to be formed from $Fe(CO)_4(C_2Cl_4)$ via a very rapid oxidative addition process. Additionally, $ClFe(CO)_4(C_2Cl_3)$ and $Fe(CO)_4(C_2Cl_4)$ would exchange places in Scheme 2. However, if the first species observed is $ClFe(CO)_4(C_2Cl_3)$, then we would not observe a second species as a result of isomerization of $ClFe(CO)_4(C_2Cl_3)$ to $Fe(CO)_4(C_2Cl_4)$, as this latter species would rapidly convert to $ClFe(CO)_4(C_2Cl_3)$. This is inconsistent with observations and confirms our assignment of species **III** as $Fe(CO)_4(C_2Cl_4)$. By implication it also confirms Haszeldine's assignment of this species.

$Fe(CO)_4(C_2Cl_4)$ exhibits a single-exponential decay at high CO/C_2Cl_4 pressure ratios (>2). The rate of this decay does not depend on ligand or parent pressure. From this behavior and the Arrhenius parameters for the process, we conclude that the decomposition pathway for this species involves isomerization of $Fe(CO)_4(C_2Cl_4)$ to $ClFe(CO)_4(C_2Cl_3)$, which then decays sufficiently rapidly that it is effectively a steady-state intermediate that is present at low concentration. The more rapid decay of the chloride than of $Fe(CO)_4(C_2Cl_4)$ is consistent with direct measurements of the lifetime of $ClFe(CO)_4(C_2Cl_3)$ when, as discussed above, it is produced by photolysis of $Fe(CO)_4(C_2Cl_4)$. For low CO/C_2Cl_4 pressure ratios (<2) and measurements made at temperatures below 304 K, the decay curve for $Fe(CO)_4(C_2Cl_4)$ is a double exponential. Under such conditions, the isomerization of this species to $ClFe(CO)_4(C_2Cl_3)$ is not the only process relevant to the disappearance of $Fe(CO)_4(C_2Cl_4)$. To understand these observations, simulations of the kinetics of the mechanism in Scheme 2 were performed using a program developed by IBM.[54] As shown in Figure 8, very good simulations of the experimental signals could be achieved for $Fe(CO)_4(C_2Cl_4)$. The simulations show that the double-exponential decay that is observed with the FTIR for $Fe(CO)_4$-

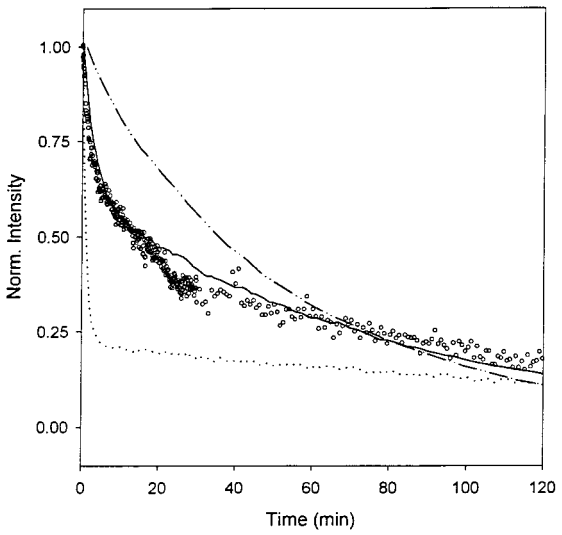

Figure 9. Plot of the results of the simulations based on Scheme 2 showing the effect of the rate constant for CO dissociation (k_d') from $Fe(CO)_4(C_2Cl_4)$ and olefin loss (k_{-L}) from $Fe(CO)_3(C_2Cl_4)_2$ on the decay of $Fe(CO)_4(C_2Cl_4)$. The signals shown were obtained at room temperature for a CO/C_2Cl_4 pressure ratio = 0.5. Open circles are the corresponding experimental signal. The solid line is for $k_d' = 1.8 \times 10^{-2}$ and $k_{-L} = 3.5 \times 10^{-3}$ s^{-1}, the dashed line is for $k_d' = 1.8 \times 10^{-2}$ and $k_{-L} = 9.6 \times 10^{-3}$ s^{-1}, and the dotted line is for $k_d' = 9.6 \times 10^{-2}$ and $k_{-L} = 3.5 \times 10^{-3}$ s^{-1}.

(C_2Cl_4) at room temperature and low CO pressure is linked principally to three processes. One of them is the equilibrium between $Fe(CO)_3(C_2Cl_4)$ and $ClFe(CO)_3(C_2Cl_3)$. To reproduce the experimental data at room temperature the equilibrium rate constant, K_{eq}, must be $\leq 10^{-3}$. This value agrees well with the estimates made in section IV.D. It is also consistent with kinetic and spectroscopic data which indicate that this equilibrium is significantly biased toward the monoolefin species. An equilibrium constant of this magnitude translates into a value for ΔG of ≥ 4 kcal/mol for the isomerization of the 16-electron species, $Fe(CO)_3(C_2Cl_4)$, to $ClFe(CO)_3(C_2Cl_3)$. The other two processes that can be associated with the fast decay of the 18-electron species, $Fe(CO)_4(C_2Cl_4)$, are the loss of CO from $Fe(CO)_4(C_2Cl_4)$ and the loss of C_2Cl_4 from the bisolefin, $Fe(CO)_3(C_2Cl_4)_2$. The outcome of the simulations was very sensitive to both the magnitude of the individual rate constants for these processes and the ratio of these rate constants. This dependence is shown in Figure 9.

Although it was found that there are at least two local minima on the multidimensional parameter surface for which the simulations fit the data at low CO pressure and 297 K, variations in the CO pressure as well as the temperature produced data that did not match the experimental data for one of these minima. The best fit to experimental data, with 2.5 Torr of CO and 5 Torr of olefin, corresponds to rate constants for loss of CO (k_d') from $Fe(CO)_4(C_2Cl_4)$ in the $(9-35) \times 10^{-3}$ s^{-1} range, *provided that the rate of loss for olefin (k_{-L}) from $Fe(CO)_3(C_2Cl_4)_2$ is 5−6 times slower*. If the rate for loss of olefin in the bisolefin product is faster than the rate of CO loss, the initial fast decay of $Fe(CO)_4(C_2Cl_4)$ is no longer evident, even for low CO/C_2Cl_4 pressure ratios and for higher temperatures. On the other hand, if the rate of loss of CO from $Fe(CO)_4(C_2Cl_4)$ is much larger than the rate of loss of olefin from $Fe(CO)_3(C_2Cl_4)_2$, the initial decay of monoolefin has a larger relative amplitude and is faster than is experimentally observed. On the basis of these simulations, it is clear that the monoolefin iron tetracarbonyl product preferentially losses CO. If a preexponential factor of 5×10^{13} s^{-1} is assumed for this process, the activation energies for CO dissociation from $Fe(CO)_4(C_2Cl_4)$ and olefin from $Fe(CO)_3(C_2Cl_4)_2$ are ∼21 kcal/mol and ∼22 kcal/mol, respectively. $Fe(CO)_3(C_2Cl_4)$ is produced via the CO loss process. This unsaturated complex can add an olefin to yield bisolefin or can isomerize to the chloride. However, the bisolefin can lose an olefin, and the chloride can isomerize back to $Fe(CO)_3(C_2Cl_4)$. Given these multiple channels, the fast decay rate is a phenomenological rate due to a combination of the microscopic kinetic processes and/or equilibria for these processes. For sufficiently low CO/C_2Cl_4 pressure ratios (Figure 8a), a relatively fast equilibrium is established between the mono- and bisolefin species through $Fe(CO)_3(C_2Cl_4)$, while $Fe(CO)_4(C_2Cl_4)$ is slowly decaying to its chloride isomer.

$$ClFe(CO)_4(C_2Cl_3) \xleftarrow{k_{iso}} Fe(CO)_4(C_2Cl_4) \underset{k_{co}'[CO]}{\overset{k_d'}{\rightleftharpoons}} Fe(CO)_3(C_2Cl_4) \underset{k_{-L}}{\overset{k_+[L]}{\rightleftharpoons}} Fe(CO)_3(C_2Cl_4)_2 \quad (27)$$

Under these conditions, an approximate analytical solution can be obtained by invoking the steady-state approximation for the $Fe(CO)_3(C_2Cl_4)$ intermediate. Using this approximation gives eqs 28 and 29, where the rates for the disappearance of $Fe(CO)_4(C_2Cl_4)$ (called M) and $Fe(CO)_3(C_2Cl_4)_2$ (called B) are

$$-d[M]/dt = (k_{iso} + k_A)[M] - k_B[B] \quad (28)$$

$$-d[B]/dt = -k_A[M] + k_B[B] \quad (29)$$

where $k_A = (k_{-d'}k_+[L])/(k_+[L] + k_{CO}'[CO])$ and $k_B = (k_{-L}k_{CO}'[CO])/(k_+[L] + k_{CO}'[CO])$.

A solution for these equations can be obtained using Laplace transforms[55] to obtain a biexponential function of the form

$$[M] = Ce^{-St} + De^{-Ut} \quad (30)$$

where

$$S = {}^1/_2\{(k_{iso} + k_A + k_B) - [(k_{iso} + k_A + k_B)^2 - 4k_{iso}k_B]^{1/2}\}$$

$$U = {}^1/_2\{(k_{iso} + k_A + k_B) + [(k_{iso} + k_A + k_B)^2 - 4k_{iso}k_B]^{1/2}\}$$

$$C = (k_B - S[M]_0)/(U - S) \text{ and } D = (U[M]_0 - k_B)/(U - S)$$

Using the experimental values for k_{CO}', k_+, and k_{iso}, as well as the k_d' and k_{-L} values from the simulation, it can be shown that the slow decay rate, S, converges to k_{iso} when the CO/C_2Cl_4 ratio is increased. Also, the fast decay rate, U, is approximately equal to the sum of k_A and k_B over the entire range of CO/C_2Cl_4 pressure ratios from 0.5 to 28, converging to k_{-L} at the high end of this range. Thus, it would, in principle, be possible to obtain k_{-L} directly from the rate of the fast decay. However, this proved to be difficult because increasing the CO/C_2Cl_4 ratio increases the ratio (C/D) of the amplitude of the slow component relative to that of the fast one. Both the simulation and the analytical solution indicate that the fast decay should have some dependence on the CO/C_2Cl_4 pressure ratio. A decrease in the rate of the fast decay of ∼19% at 304 K and 25% at 294 K is predicted in going from a CO/C_2Cl_4 pressure ratio of 0.5 to a ratio of 2. As previously mentioned, the error in the determination of the rate for the fast decay is about 20−30% for such a ratio, with errors becoming larger as the CO pressure is increased, because the amplitude of the fast component decreases. Given that the experimental error in the determination is of the same magnitude as the predicted change, it is not surprising that it was not possible to accurately

determine the CO dependence of the fast component. For the same reason, the temperature dependence of the fast decay could not be determined. According to the simulation and analytical results, a temperature dependence is expected because the decay depends on k_d' and k_{-L}, which are expected to be temperature-dependent. As the temperature decreases, the amplitude of the fast decay becomes larger because the isomerization reaction slows, and the monoolefin−bisolefin preequilibrium dominates the decay. At higher temperatures, the isomerization rate becomes comparable to the rate of establishment of the equilibrium, and as can be seen in Figure 8c, the fast decay is no longer observable.

When a relatively high pressure of CO is present, $Fe(CO)_3(C_2Cl_4)$ can add CO fast enough that the CO addition/dissociation equilibrium is pushed toward formation of $Fe(CO)_4(C_2Cl_4)$, making the effect of the CO dissociation process insignificant. When this occurs, only a single decay is observed, and this decay of $Fe(CO)_4(C_2Cl_4)$ effectively corresponds to isomerization (Figure 8b and 8d), as indicated by the simulations as well as the analytical solution (S converges to k_{iso}).

The range of the parameters in the simulations that lead to the best fit to experimental data indicate that at room temperature, $Fe(CO)_3(C_2Cl_4)_2$ has an intrinsic lifetime of ∼2−9 min. However, because the bisolefin is involved in an equilibrium with the monoolefin, its actual lifetime under experimental conditions is longer, and because of the equilibrium between the bis- and monoolefins, the decay of $Fe(CO)_3(C_2Cl_4)_2$ should match the decay of the monoolefin. The simulations also indicate that the post-photolysis concentration of bisolefin at CO/C_2Cl_4 ratios >0.2 is at least 5 times smaller than that of the monoolefin. This predicted behavior helps explain the difficulty in detecting the bisolefin at CO/C_2Cl_4 ratios >0.2. The more intense bands of $Fe(CO)_4(C_2Cl_4)$ overlap those of $Fe(CO)_3(C_2Cl_4)_2$ while both compounds decay at the same rate. The optimum conditions for observing $Fe(CO)_3(C_2Cl_4)_2$ is for CO/C_2Cl_4 ratios of <0.2. Under these conditions, the bisolefin grows to a maximum and then decays slowly, while the monoolefin rapidly decays to a lower concentration. However, even under these conditions, the maximum concentration of $Fe(CO)_3(C_2Cl_4)_2$ is not predicted to be large. Data in Figure 10 are taken for CO/C_2Cl_4 ratios <0.2. Given the constraints imposed by the limited signal-to-noise levels, the ability of simulations to reproduce the experiment is considered satisfactory.

V. Conclusions

The rate constants for the addition of C_2Cl_4 to $Fe(CO)_4$ and $Fe(CO)_3$ have been measured as $(1.2 \pm 0.3) \times 10^{-13}$ and $(3.0 \pm 0.8) \times 10^{-11}$ cm^3 molecule^{-1} s^{-1}, respectively, at 25 °C. These rate constants are smaller than those for the corresponding addition reactions with ethylene as the adduct.[10] The $Fe(CO)_4(C_2Cl_4)$ monoolefin complex is formed by the addition of tetrachloroethylene to iron tetracarbonyl. Gas-phase absorptions for this complex have been observed at 2039, 2069, and 2125 cm^{-1} and correspond well with those observed for this species in solution.[16] $Fe(CO)_4(C_2Cl_4)$ can isomerize to a perchlorovinyl iron tetracarbonyl chloride complex [$ClFe(CO)_4(C_2Cl_3)$] via an oxidative addition process. The energy of activation and preexponential factor for the isomerization involving the $Fe(CO)_4(C_2Cl_4)$ monoolefin complex are consistent with those previously reported for an analogous reaction in a platinum(0) complex.[34] Analogous oxidative addition processes have also been previously observed in some manganese and iron complexes.[14−20] Using known and estimated bond energies, we conclude that this type of transformation is thermodynamically more favorable in $Fe(CO)_4(C_2Cl_4)$ than for the corresponding ethylene and perfluoroethylene complexes. However, $ClFe(CO)_4(C_2Cl_3)$ is not directly observed when produced via this isomerization pathway because it decays faster than $Fe(CO)_4(C_2Cl_4)$ isomerizes to $ClFe(CO)_4(C_2Cl_3)$.

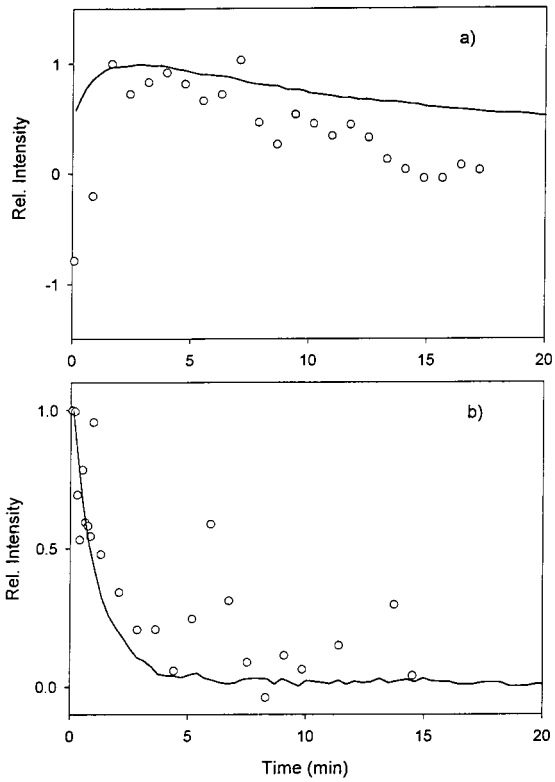

Figure 10. Data for the time evolution of (a) $Fe(CO)_3(C_2Cl_4)_2$ and (b) $Fe(CO)_4(C_2Cl_4)$ without added CO. Open circles are experimental data, and the lines are the result of a simulation using $P_{CO} = 0.07$ Torr [from $Fe(CO)_5$ photolysis] and 5.0 Torr of olefin.

When a sample of $Fe(CO)_5$ and C_2Cl_4 is photolyzed in a large excess of added CO, a species with absorptions at 2089, 2109, and 2166 cm^{-1} is detected. This species is formed by rearrangement of $Fe(CO)_3(C_2Cl_4)$, which is formed by photolytic loss of a CO from $Fe(CO)_4(C_2Cl_4)$. The species thus formed is best identified as $ClFe(CO)_4(C_2Cl_3)$, which is also the product of the isomerization of $Fe(CO)_4(C_2Cl_4)$ discussed above. To our knowledge, $ClFe(CO)_4(C_2Cl_3)$ has not been previously reported.

However, we cannot completely exclude the possibility that the observed compound (**IV**) is $Fe(CO)_4(Cl)_2$, which would have $ClFe(CO)_3(C_2Cl_3)$ as a precursor and form as a result of a second chlorine transfer reaction followed by elimination of dichloroacetylene. CO addition could occur either before or after the second chlorine transfer process and C_2Cl_4 elimination. Direct observation of the chloride complex demonstrates that, as expected, it decays much faster than $Fe(CO)_4(C_2Cl_4)$ by what are likely heterogeneous reactions taking place at the cell walls.

Irrespective of the identity of the chloride, its formation is explained only if an oxidative addition reaction involving chlorine migration occurs in the unsaturated $Fe(CO)_3(C_2Cl_4)$ complex with a rate that is at least comparable to that for addition of any ligand. This places a *lower limit* on the rate of this process of 6×10^6 s^{-1}. The rate constants for addition of CO and C_2Cl_4 to $Fe(CO)_3(C_2Cl_4)$, which has an absorption at 2076 cm^{-1}, are $(2.4 \pm 0.7) \times 10^{-12}$ and $(1.9 \pm 0.3) \times 10^{-13}$ cm^3 molecule^{-1} s^{-1}, respectively, at 24 °C. The rate constant for addition of C_2Cl_4 to $Fe(CO)_3(C_2Cl_4)$, which is "abnormally" small when compared to the rate constant for addition of CO

and of other C_2X_4 (X = H, F) species to $Fe(CO)_3(C_2X_4)$, could be the result of the equatorially bound C_2Cl_4 sterically hindering the approach of another C_2Cl_4 ligand. To our knowledge, $Fe(CO)_3(C_2Cl_4)_2$, which has absorptions at 2057 and 2084 cm^{-1}, has not been previously observed.

Scheme 2 is a mechanism that describes the formation and decay of the species detected following the reactions of $Fe(CO)_3$, $Fe(CO)_4$, and $Fe(CO)_3(C_2Cl_4)$ with C_2Cl_4. Simulations of the kinetics inherent in this mechanism generate signals that agree well with the observed behavior of $Fe(CO)_4(C_2Cl_4)$. From these simulations, ΔG for the isomerization of $Fe(CO)_3(C_2Cl_4)$ to its chloride isomer is estimated to be ≥ 4 kcal/mol at 297 K, indicating that $Fe(CO)_3(C_2Cl_4)$ is thermodynamically favored relative to $ClFe(CO)_3(C_2Cl_3)$. The biexponential decay of $Fe(CO)_4(C_2Cl_4)$, observed at low CO/C_2Cl_4 pressure ratios (<2), can be reproduced with these simulations, as well as with an approximate analytical solution for the relevant decay kinetics. The fast decay of $Fe(CO)_4(C_2Cl_4)$ involves an equilibrium between the monoolefin and the bisolefin, with $Fe(CO)_3(C_2Cl_4)$ as the intermediate. CO dissociation from $Fe(CO)_4(C_2Cl_4)$ is preferred over olefin dissociation, although permanent CO loss is not the main decay path for $Fe(CO)_4(C_2Cl_4)$ under experimental conditions. However, if $Fe(CO)_4(C_2Cl_4)$ could be produced in the absence of CO, the CO loss channel would then be a dominant decay pathway.

The activation energy for the isomerization of $Fe(CO)_4(C_2Cl_4)$ to $ClFe(CO)_3(C_2Cl_3)$ has been determined to be 21 ± 2 kcal/mol. This isomerization process is the rate-limiting step in a series of reactions that leads to decomposition of the initially formed $Fe(CO)_4(C_2Cl_4)$ complex. The BDE's for the $Fe-C_2Cl_4$ and the $CO-Fe(CO)_3(C_2Cl_4)$ bonds are expected to be at least ~22 kcal/mol.

Comparisons of these results with those obtained for iron carbonyl complexes of ethylene and perchloroethylene demonstrate how the nature of the atoms attached to the carbons in the olefin ligand(s) can influence the bonding and thermochemistry of a complex. These factors can, in turn, affect the rate constants and reaction pathways available to these compounds.

Acknowledgment. We acknowledge support of this work by the National Science Foundation under Grant CHE97-34891.

References and Notes

(1) Collman, J. P.; Hegedus, L. S.; Norton, J. R.; Finke, R. G. *Principles and Applications of Organotransition Metal Chemistry*; University Science Books: Mill Valley, CA, 1987.

(2) Crabtree, R. H. *The Organometallic Chemistry of Transition Metals*; Wiley: New York, 1994.

(3) Yamamoto, A. *Organotransition Metal Chemistry*; Wiley: New York, 1986.

(4) Geoffroy, G. L.; Wrighton, M. S. *Organometallic Photochemistry*; Academic Press: New York, 1979.

(5) Wells, J. R.; Weitz, E. *J. Phys. Chem.* **1993**, *97*, 3084.

(6) Dewar, M. J. S. *Bull. Chem. Soc. Fr.* **1951**, *18*, C79.

(7) Chatt, J.; Duncanson, L. A. *J. Chem. Soc.* **1953**, 2939.

(8) Weitz, E. *J. Phys. Chem.* **1994**, *98*, 11256.

(9) Weitz, E. In *Energetics of Stable Molecules and Reactive Intermediates*, Minas de Piedade, M. E., Ed.; Kluwer Academic Publishers: Norwell, MA, 1999; p 215.

(10) House, P. G.; Weitz, E. *J. Phys. Chem. A* **1997**, *101*, 2988.

(11) Wang, W.; Weitz, E. Unpublished data. DFT calculations were performed using effective core potential basis set and both BP86 and B3LYP functionals.

(12) Bland, W. J.; Kemmitt, R. D. W. *J. Chem. Soc. A* **1968**, 1278.

(13) Bland, W. J.; Burgess, J.; Kemmitt, R. D. W. *J. Organomet. Chem.* **1968**, *14*, 201.

(14) Wilford, J. B.; Forster, A.; Stone, F. G. A. *J. Chem. Soc.* **1965**, 6519.

(15) Fields, R.; Germain, M. M.; Haszeldine, R. N.; Wiggans, P. W. *J. Chem. Soc. A* **1970**, 1969.

(16) Fields, R.; Godwin, G. L.; Haszeldine, R. N. *J. Organomet. Chem.* **1971**, *26*, C70.

(17) Fields, R.; Godwin, G. L.; Haszeldine, R. N. *J. Chem. Soc., Dalton Trans.* **1975**, 1867.

(18) Grevels, F. W.; Schulz, D.; Koerner von Gustorf, E.; Bunbury, D. St. P. *J. Organomet. Chem.* **1975**, *91*, 341.

(19) Nelson, S. M.; Regan, C. M.; Sloan, M. *J. Organomet. Chem.* **1975**, *96*, 383.

(20) Löwe, C.; Hund, H.; Berke, H. *J. Organomet. Chem.* **1989**, *372*, 295.

(21) Seder, T. A., Ouderkirk, A. J.; Weitz, E. *J. Chem. Phys.* **1986**, *85*, 1977.

(22) Ryther, R. J.; Weitz, E. *J. Phys. Chem.* **1992**, *96*, 2561.

(23) (a) Noack, K. *Helv. Chim. Acta* **1962**, *45*, 1847. (b) Taylor, R. C.; Horrocks, W. D., Jr. *Inorg. Chem.* **1964**, *3*, 584.

(24) Le Bras, J.; Amouri, H.; Vaissermann J. *J. Organomet. Chem.* **1997**, *548*, 305.

(25) (a) Noack, K. *J. Organomet. Chem.* **1968**, *13*, 411. (b) Johnson, B. F. G.; Lewis, J.; Robinson, P. W.; Miller, J. R. *J. Chem. Soc. A* **1968**, 1043.

(26) Weiller, B. H.; Miller, M. E.; Grant, E. R. *J. Am. Chem. Soc.* **1987**, *109*, 352.

(27) Jordan, R. B. *Reaction Mechanisms of Inorganic and Organometallic Systems*; Oxford University Press: New York, 1991.

(28) (a) Rossi, A. R.; Hoffmann, R. *Inorg. Chem.* **1975**, *14*, 365. (b) Elian, M.; Hoffmann, R. *Inorg. Chem.* **1975**, *14*, 1058.

(29) Angermund, H.; Grevels, F. W.; Moser, R.; Benn, R.; Kruger, C.; Romao, M. J. *Organometallics* **1988**, *7*, 1994.

(30) Grevels, F. W.; Jacke, J.; Klotzbucher, W. E.; Oskar, S.; Skibbe, V. *Pure Appl. Chem.* **1988**, *60*, 1017. (b) von Buren, M.; Cosandey, M.; Hansen, H. J. *Helv. Chim. Acta* **1980**, *63*, 738. (c) Wilson, S. T.; Coville, N. J.; Shapely, J. R.; Osborn, J. A. *J. Am. Chem. Soc.* **1974**, *96*, 4038. (d) Kruczynski, L.; LiShingMan, K. K.; Takats, J. *J. Am. Chem. Soc.* **1974**, *96*, 4006.

(31) Stoutland, P. O.; Bergman, R. G. *J. Am. Chem. Soc.* **1988**, *110*, 5732.

(32) Baker, M. V.; Field, L. D. *J. Am. Chem. Soc.* **1986**, *108*, 7436.

(33) Benson, S. W. *The Foundations of Chemical Kinetics*; McGraw-Hill: New York, 1960.

(34) Bland, W. J.; Burgess, J.; Kemmitt, R. D. W. *J. Organomet. Chem.* **1968**, *15*, 217.

(35) Seetula, J. A. *J. Chem. Soc., Faraday Trans.* **1998**, *94*, 1933.

(36) Hildenbrand, D. L. *J. Chem. Phys* **1995**, *103*, 2634.

(37) Nolan, S. P.; Hoff, C. D.; Stoutland, P. O.; Newman, L. J.; Buchanan, J. M.; Bergman, R. G.; Yang, G. K.; Peters, K. S. *J. Am. Chem. Soc.* **1987**, *109*, 3143.

(38) Wang, W.; Narducci, A. A.; House, P. G.; Weitz, E. *J. Am. Chem. Soc.* **1996**, *118*, 8654.

(39) Lewis, K. E.; Golden, D. M.; Smith, G. P. *J. Am. Chem. Soc.* **1984**, *106*, 3905.

(40) (a) Wuu, Y.; Bentsen, J. G.; Brinkley, C. G.; Wrighton, M. S. *Inorg. Chem.* **1987**, *26*, 530. (b) Mitchener, J. C.; Wrighton, M. S. *J. Am. Chem. Soc.* **1983**, *105*, 1065.

(41) Wells, J. R.; House, P. G.; Weitz, E. *J. Phys. Chem.* **1994**, *98*, 8343.

(42) Davis, M. I.; Speed, C. S. *J. Organomet. Chem.* **1970**, *21*, 401.

(43) Beagley, B.; Schmidling, D. G.; Cruickshank, D. W. J. *Acta Crystallogr.* **1973**, *B29*, 1499.

(44) Barnhart, T. M.; Fenske, R. F.; McMahon, R. J. *Inorg. Chem.*, **1992**, *31*, 2679.

(45) (a) Kaslauskas, R. J.; Wrighton, M. S. *J. Am. Chem. Soc.* **1982**, *104*, 6005. (b) Mahmoud, K. A.; Rest, A. J.; Alt, H. G.; Eichner, M. E.; Jansen, B. M. *J. Chem. Soc., Dalton Trans.* **1984**, 175. (c) Yang, G. K.; Peters, K. S.; Vaida, V. *J. Am. Chem. Soc.* **1986**, *108*, 2511.

(46) Long, G. T.; Wang, W.; Weitz, E. *J. Am. Chem. Soc.* **1995**, *117*, 12810.

(47) Heck, R. F.; Boss, C. R. *J. Am. Chem. Soc.* **1964**, *86*, 2580.

(48) Ghosh, C. K.; Hoyano, J. K.; Krentz, R.; Graham, W. A. G. *J. Am. Chem. Soc.* **1989**, *111*, 5480.

(49) House, P. G.; Weitz, E. *Chem. Phys. Lett.* **1997**, *266*, 239.

(50) Seder, T. A.; Ouderkirk, A. J.; Weitz, E. *J. Chem. Phys.* **1977**, *85*, 1977.

(51) Poliakoff, M.; Weitz, E. *Acc. Chem. Res.* **1987**, *20*, 408.

(52) Sybyl version 6.0; Tripos Inc.: St. Louis, MO.

(53) Ryther, R. J.; Weitz, E. *J. Phys. Chem.* **1991**, *95*, 9841.

(54) *Chemical Kinetics Simulations*, Version 1.0.1 for Windows; IBM Research Corp.: Armonk, NY.

(55) Steinfeld, J. I.; Francisco, J. S.; Hase, W. L. *Chemical Kinetics and Dynamics*; Prentice Hall: New York, 1989.